Article

Immunity

Dietary Fatty Acids Directly Impact Central Nervous System Autoimmunity via the Small Intestine

Highlights

- Dietary fatty acids have profound influence on T cell differentiation in the gut
- Middle- and long-chain fatty acids (LCFAs) support Th1 and Th17 cell differentiation
- Short-chain fatty acids (SCFAs) lead to increased Treg cell differentiation
- LCFAs worsen disease in an animal model of MS; SCFAs exert the opposite effect

Authors

Aiden Haghikia, Stefanie Jörg, Alexander Duscha, ..., Dominik N. Müller, Ralf Gold, Ralf A. Linker

Correspondence

aiden.haghikia@rub.de (A.H.), ralf.linker@uk-erlangen.de (R.A.L.)

In Brief

Haghikia and colleagues show that dietary fatty acids (FAs) influence T cell differentiation in the gut, with short FAs leading to increased Treg cell differentiation and long FAs supporting Th1 and/or Th17 cell differentiation. These FAs differentially affect EAE severity, demonstrating a direct dietary impact on central nervous system autoimmunity.

Haghikia et al., 2015, Immunity *43*, 817–829
October 20, 2015
http://dx.doi.org/10.1016/j.immuni.2015.09.007

CellPress

Immunity
Article

Dietary Fatty Acids Directly Impact Central Nervous System Autoimmunity via the Small Intestine

Aiden Haghikia,[1,10,*] Stefanie Jörg,[2,10] Alexander Duscha,[1] Johannes Berg,[1] Arndt Manzel,[2] Anne Waschbisch,[2] Anna Hammer,[2] De-Hyung Lee,[2] Caroline May,[3] Nicola Wilck,[4] Andras Balogh,[4] Annika I. Ostermann,[5] Nils Helge Schebb,[5,6] Denis A. Akkad,[7] Diana A. Grohme,[8] Markus Kleinewietfeld,[8] Stefan Kempa,[9] Jan Thöne,[1] Seray Demir,[1] Dominik N. Müller,[4] Ralf Gold,[1,11] and Ralf A. Linker[2,11,*]
[1]Department of Neurology, Ruhr-University Bochum, 44801 Bochum, Germany
[2]Department of Neurology, Friedrich-Alexander-University Erlangen-Nuremberg, 91054 Erlangen, Germany
[3]Medical Proteom-Center, Ruhr-University Bochum, 44801 Bochum, Germany
[4]Experimental and Clinical Research Center & Max-Delbrück Center Berlin, 13125 Berlin, Germany
[5]Institute for Food Toxicology and Analytical Chemistry, University of Veterinary Medicine Hannover, 30559 Hannover, Germany
[6]Department of Food Chemistry, University of Wuppertal, 42097 Wuppertal, Germany
[7]Department of Human Genetics, Ruhr-University Bochum, 44801 Bochum, Germany
[8]Translational Immunology, Medical Faculty Carl Gustav Carus, TU Dresden, 01307 Dresden, Germany
[9]Integrative Metabolomics and Proteomics, Berlin Institute of Medical Systems Biology/Max-Delbrück Center for Molecular Medicine, 13125 Berlin, Germany
[10]Co-first author
[11]Co-senior author
*Correspondence: aiden.haghikia@rub.de (A.H.), ralf.linker@uk-erlangen.de (R.A.L.)
http://dx.doi.org/10.1016/j.immuni.2015.09.007

SUMMARY

Growing empirical evidence suggests that nutrition and bacterial metabolites might impact the systemic immune response in the context of disease and autoimmunity. We report that long-chain fatty acids (LCFAs) enhanced differentiation and proliferation of T helper 1 (Th1) and/or Th17 cells and impaired their intestinal sequestration via p38-MAPK pathway. Alternatively, dietary short-chain FAs (SCFAs) expanded gut T regulatory (Treg) cells by suppression of the JNK1 and p38 pathway. We used experimental autoimmune encephalomyelitis (EAE) as a model of T cell-mediated autoimmunity to show that LCFAs consistently decreased SCFAs in the gut and exacerbated disease by expanding pathogenic Th1 and/or Th17 cell populations in the small intestine. Treatment with SCFAs ameliorated EAE and reduced axonal damage via long-lasting imprinting on lamina-propria-derived Treg cells. These data demonstrate a direct dietary impact on intestinal-specific, and subsequently central nervous system-specific, Th cell responses in autoimmunity, and thus might have therapeutic implications for autoimmune diseases such as multiple sclerosis.

INTRODUCTION

Renewed focus on the gut, the largest zone of interaction between the environment and the human organism, has opened new avenues for various fields of life sciences engaged in health and disease. A rapid and simultaneous paradigm shift in microbiologic diagnostics from classical culturing to next-generation sequencing has enabled a more precise estimation of the human gut microbiome composition under healthy conditions (Lozupone et al., 2012). Consequently, there is fast-growing quest for possible disease associations involving interactions between diet, the gut, and microbiome components, especially in autoimmunity (e.g., diabetes and inflammatory bowel disease [IBD]) (Brown et al., 2013; Clemente et al., 2012).

In spite of many remaining questions regarding which components of the microbiome are critically responsible for the fine-tuning of adaptive immune responses in the gut, growing empirical evidence suggests that nutrition and bacterial metabolites might impact the systemic immune response in the context of disease and autoimmunity (Cotillard et al., 2013; Macia et al., 2012). Here, fatty acids (FAs), as an integral component of daily diet, have become a primary focus of investigation. Of particular interest is the role of short-chain FAs (SCFAs), which are solely metabolized by gut bacteria from otherwise indigestible carbohydrates, i.e., from fiber-rich diets, and have been shown to ameliorate disease in models of IBD and allergic asthma (Smith et al., 2013; Trompette et al., 2014). Further, long-chain FAs (LCFAs), the most abundant component of the so-called Western diet, have been suspected as a culprit in various diseases. Although extensive data on the effects of saturated FAs on the innate immune system exist from the field of cardiovascular disease, their impact on the players of the adaptive immune system is less well understood (Bhargava and Lee, 2012). Although the downstream mechanisms and the cellular mediators for the effect of SCFAs remain inconclusive, most data point to the involvement of regulatory immune mechanisms. For example, in models of IBD, gavage of various SCFAs leads to local

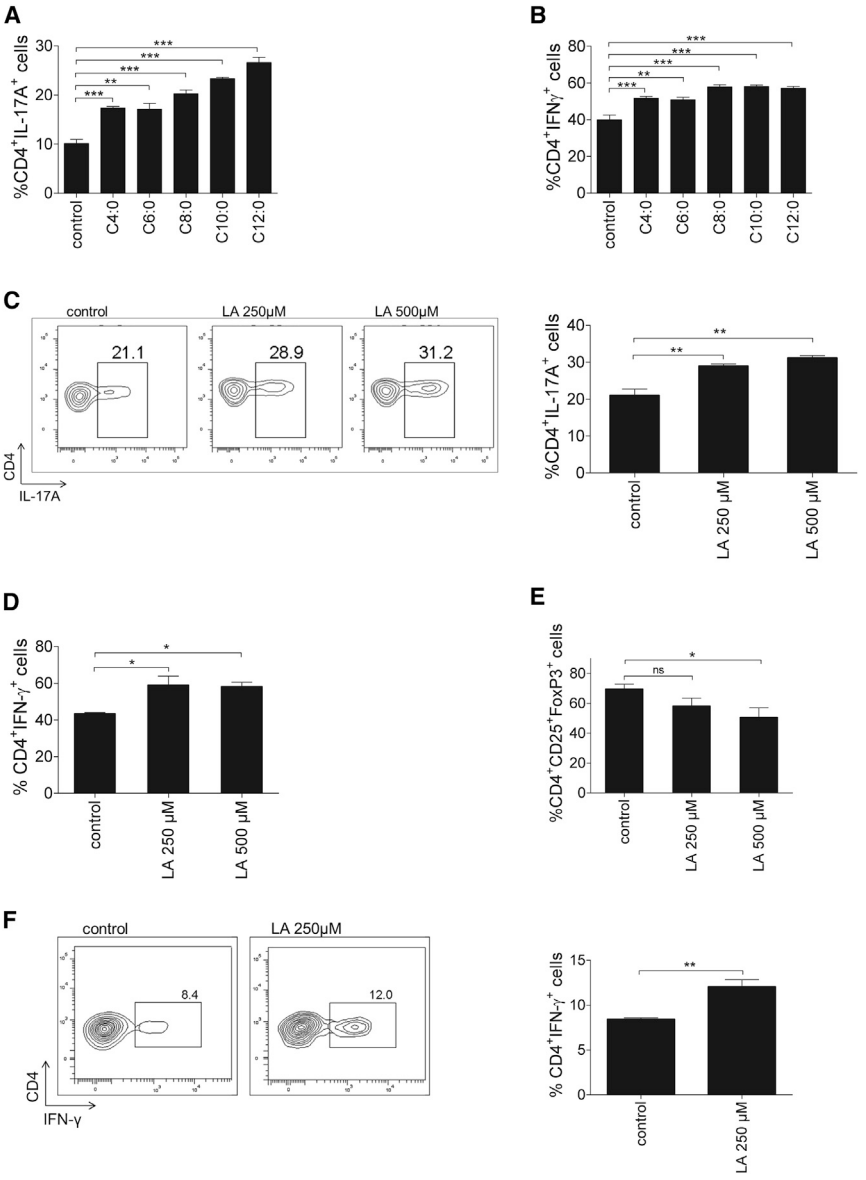

Figure 1. LCFAs Promote Polarization of Naive T Cells toward Th1 and Th17 Cells

(A and B) Addition of FA derivatives to murine CD4$^+$ T cell differentiation culture under Th17 (A) and Th1 (B) cell polarizing conditions. C4:0 butyric acid, C6:0 caproic acid, C8:0 caprylic acid, C10:0 capric acid, C12:0 LA (all at 250 μM; n = 3, one out of two representative experiments shown).

(C and D) Addition of LA to murine CD4$^+$ T cell differentiation culture under Th17 (C) and Th1 (D) cell polarizing conditions (n = 6, data pooled from two experiments, *p < 0.05).

(E) Addition of LA to murine CD4$^+$ T cell differentiation culture under Treg cell polarizing conditions (n = 6, data pooled from two experiments).

(F) Addition of LA to human CD4$^+$ T cell differentiation culture under Th1 cell polarizing conditions (n = 5, one out of two experiments shown).

*p < 0.05, **p < 0.01. See also Figure S1. For all figures, data are given as mean ± SEM, unless annotated otherwise.

expansion of intestinal T regulatory (Treg) cells (Smith et al., 2013; Furusawa et al., 2013), and microbiome analyses of a large cohort of affected individuals with type 2 diabetes revealed a lack of butyrate-producing bacteria, further underscoring the impact of FAs in health and disease (Qin et al., 2012).

The gut microbiome, along with various dietary habits such as high salt intake, has been recently established as an environmental contributor to the pathogenesis of multiple sclerosis (MS) (Berer et al., 2011; Kleinewietfeld et al., 2013), a T-cell-mediated autoimmune disease of the central nervous system (CNS) with neurodegenerative features (Haghikia et al., 2013). Previous interdisciplinary research has led to the contemporary view that the autoimmune basis of MS stems from an imbalance between pathogenic pro-inflammatory Th1 and/or Th17 cells and anti-inflammatory or regulatory mechanisms of immune cells including Treg cells (Kleinewietfeld and Hafler, 2014). Thus, the rationale of currently available therapeutic interventions is to suppress pathogenic Th1 and Th17 cells and/or to augment Treg cell differentiation (Haghikia et al., 2013).

Here, we show that dietary-induced changes in the gut shaped Th cell responses through the opposing effects of dietary SCFAs and the less-well-studied medium-chain (MC) FAs or LCFAs.

RESULTS

LCFAs Promote Polarization of Naive T Cells toward Th1 and Th17 Cells

To investigate effects of alkanoic acids on the differentiation of naive T cells under Th1 and Th17 cell polarizing conditions in vitro, we tested derivatives with different aliphatic chain lengths in murine CD4$^+$ T cells (Figures 1A and 1B). At 250–500 μM, the C12 FA dodecanoic acid (lauric acid [LA]) increased differentiation of Th17 cells (Figure 1C) and Th1 cells (Figure 1D) by ~50% as compared to control conditions; LA decreased the differentiation of CD4$^+$CD25$^+$ Foxp3$^+$ Treg cells by about one third versus control (Figure 1E). Growth curves and apoptosis rates did not differ between controls and LA-treated cultures, indicating that LA acted to directly enhance T cell differentiation and did not merely affect T cell expansion or viability (Figures S1A–S1L). The addition of LA versus control to naive (CD45RA$^+$CD45RO$^-$CD127$^+$CD25$^-$) CD4$^+$ T cells from healthy human donors also increased the differentiation of CD4$^+$interferon-γ$^+$ (IFN-γ) T cells by about 35% (Figure 1F). Expression analyses of differentiated T cell gene signatures revealed increased mRNA expression of *Ifng*, granulocyte macrophage colony-stimulating factor (*Csf2*), and tumor necrosis factor alpha (*Tnf*), but not interleukin-17A (*Il17a*) for Th1 cells (Figure S2A). Congruent analyses also revealed increased mRNA levels of *Il17a*, *Csf2*, *Rorc*, aryl hydrocarbon

receptor (*Ahr*), *Tbx21*, *Il23a*, IL-23 receptor (*Il23r*), transforming growth factor beta (*Tgfb1*), and *Tnf*, but not *Ifng*, in the presence of 250 μM LA versus control (Figure S2B), supporting the argument for an increased generation of Th17 cells after addition of LA in vitro. Treg cell quantitative real-time PCR (qRT-PCR) revealed a ~50% reduction of *Foxp3* expression after addition of LA versus control in vitro (Figure S2C).

Gene and Protein Expression Analyses Implicate Th17 Cell and MAPK Pathways as Modulators of LA Cellular Mechanism

To further understand the differential effects of different FA lengths on T cell differentiation, we analyzed gene expression of the candidate fatty acid receptors liver X receptor alpha (LXRα) and various G protein coupled receptors (GPR40, GPR41, GPR43, GPR84, GPR119, and GPR120) in different $CD4^+$ T cell subsets. The presence of GPR40, 41, 43, and 84 on the mRNA level was mostly confined to naive T cells. In contrast to previous reports (Smith et al., 2013), none of the receptors were detectable in Th17 cells or Treg cells, and only *Gpr43* was present in Th1 cells. *Lxra*, *Gpr119*, and *Gpr120* were not detected in any T cell subset (Figure S2D). Likewise, addition of the Toll-like receptor 1/2 agonist Pam3CSK4 to Th1, Th17, or Treg cell differentiation assays did not show any comparable effect to LA (not shown).

No additional increase of Th17 cell frequency was found subsequent to the addition of LA to dendritic cells (DCs) cocultured with LA-treated T cells, arguing for a direct effect of LA in fostering Th17 cell polarization (Figure 2A). In order to identify downstream signaling factors potentially involved in the LA effect on Th17 cell differentiation, we evaluated the transcriptome profile of in vitro, LA-treated versus -untreated Th1 and Th17 cells. Analyses of Th17 cells revealed *Maf* (*c-Maf*) as the highest differentially expressed gene (DEG), increasing 16.5-fold in LA- versus control-treated T cells (Figure 2B). Further DEGs pointing to induction of Th17 cell differentiation in multiple pathway analyses included the salt-sensing kinase *Sgk1* and multiple MAPK family members, such as *Mapk14* (encodes p38). The expression profile of Th1 cells revealed differential expression of critical Th1 cell genes, whereas changes in the MAPK family were not as prominent (not shown).

Because p38 MAPK-mediated signaling is a well-characterized integrator of environmental stressors, we tested the effects of FAs on p38 MAPK regulation. Expression analysis revealed a statistically significant ~13-fold increase in *Mapk14* in Th17 cells, and to a lesser degree in Th1 cells, upon LA application (Figure 2C). At the post-transcriptional level, LA treatment of T cells under Th17-cell-polarizing conditions led to a significant increase of p38 phosphorylation (pp38, Figure 2D). Pharmacological inhibition of p38 MAPK via addition of the specific blocker SB202190 almost completely inhibited the effect of LA on Th17 or Th1 cell polarization (Figures 2E and 2F). Furthermore, genetic ablation of the p38α subunit via CD4-cre-mediated deletion in T cells completely abolished the enhanced Th17 and Th1 cell differentiation effect of LA (Figures 2G and 2H). Neither pharmacological inhibition nor genetic ablation of p38 led to increased cell death (not shown).

SCFAs Promote Polarization of Naive T Cells toward Treg Cells

Corresponding to the effect of FAs on Th1 and Th17 cell differentiation, we tested derivatives with different aliphatic chain lengths on naive T cells under Treg-cell-polarizing conditions (Figures 3A and 3B). Propionate (PA, C3:0) revealed the most significant effect on murine Treg cell differentiation in vitro at a concentration of 150 μM (Figure 3C). We further corroborated the Treg-cell-stimulating effect of PA in vitro in a human T cell differentiation assay. Therein, application of PA to healthy donor naive $CD4^+$ T cells increased both the frequency of $CD4^+CD25^+$ $Foxp3^+$ cells and, to a lesser extent, the proliferation of differentiated Treg cells (Figure 3D). Adding PA to human naive T cells under Th17-cell-polarizing conditions led to a significant reduction in the frequency of $CD4^+$IL-$17A^+$ T cells (Figure 3E).

Furthermore, ex vivo transcriptome analyses of Treg cells derived from PA-pre-treated mice and Treg cells from previously untreated mice revealed DEGs in the two different cell populations (Figure 3F). Through the use of multiple pathway analyses steps, rationally selected DEGs revealed, and qRT-PCR confirmed (Figure 3G), *Lpin-2* (encodes lipin2) and Mapk8 interacting protein-2 (*Mapk8ip2*, encodes JIP2) as relevant, upregulated genes in Treg cells from PA-pre-treated mice. In contrast, LA treatment led to a downregulation of *Lpin-2* expression in both Th1 and Treg cells; however, changes in *Mapk8ip2* were not significant in both cell types. Furthermore, LA treatment had no effect on this pathway in Th17 cells. As previously shown, the increase of *Lpin-2* led downstream to downregulation of JNK1 activation (encoded by *Mapk8*), which in turn is a key activator of pro-inflammatory transcription factors such as NF-κB. Relative mRNA expression of *Mapk8* parallels that of *Lpin-2* in all investigated cell types after LA application (Figures S3A–S3C). At the post-transcriptional level, PA treatment of T cells led to an opposing effect on p38 phosphorylation (pp38, Figure 3H) compared to that which was exerted by LA on Th17 cells (Figure 2D).

LA-Rich Diet Impacts Th1-Cell- and Th17-Cell-Mediated CNS Autoimmunity In Vivo

The distinct in vitro effects of FAs on naive $CD4^+$ cells prompted us to examine their effects in vivo using murine MOG_{35-55} EAE as a model of Th1-cell- and/or Th17-cell-mediated autoimmunity. Male C57BL/6 mice were fed standardized and otherwise completely matched diets rich in either LA (C12) or palmitic acid (PALM, C16) and were compared to mice on a control diet after EAE induction. Mice on the LA-rich diet did not display different body weights compared to controls (mean ± SEM on day 20 of EAE: 22.2 ± 0.5 g versus 23.8 ± 2.0 g, $p = 0.96$). Mice fed the LA-/PALM-rich diets displayed a more severe course of the disease (Figures 4A and S4A–S4C), although disease incidence (12/13 ctrl. versus 10/10 LA) and mortality were unaffected. Upon ex vivo phenotyping by flow cytometry of the spinal cord infiltrates, the LA diet increased Th17 cell frequencies in the CNS on day 14 post immunization (p.i.) whereas Th1 cells (Figure 4B) and $CD11b^+$ antigen-presenting cells (Figure 4C) remained unchanged.

Phenotyping of splenic T cells during EAE revealed an increase of Th1 and Th17 cell frequencies under an LA-rich diet on day 10 p.i. (Figure 4D). In parallel, an LA-rich diet expanded

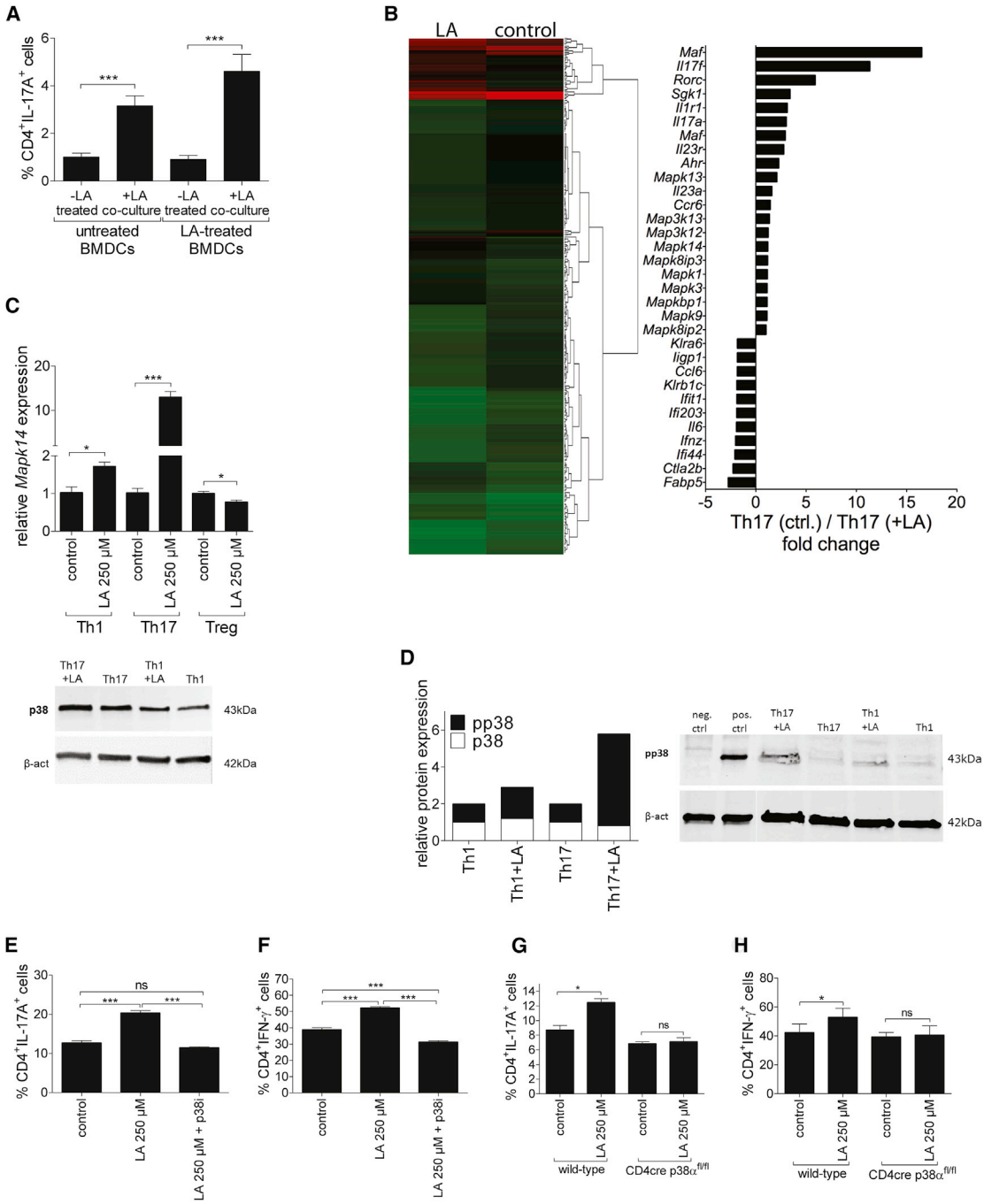

Figure 2. MAPK Pathways Are Modulators of LA Cellular Mechanism

(A) Addition of LA to co-culture assay of T cells and dendritic cells generated in the presence (LA-treated BMDCs) or absence (untreated BMDCs) of 250 μM LA (n = 3, one out of three independent experiments shown).

(B) Microarray analysis of in-vitro-generated Th17 cells in the presence (Th17+LA) or absence (Th17 ctrl) of 250 μM LA. Left: Heat map analysis displaying differentially expressed genes (DEG). Right: a selection of 32 up- and downregulated genes.

(C) Gene expression analysis of *Mapk14* (p38 MAPK) expression in Th1, Th17, and Treg cell differentiation assays (triplicates, data pooled from two preparations).

(D) Immunoblot analysis of p38 protein and phosphorylated p38 protein (pp38) in Th1 and Th17 cell differentiation assays with and without LA. Left: quantification of p38 and pp38 protein. Right: representative blots. β-actin (β-act) was used as loading control.

(E and F) Chemical inhibition of p38 via the addition of SB202190 to murine $CD4^+$ T cell differentiation culture under Th17 (E) and Th1 (F) cell polarizing conditions (n = 4–7 per group, data pooled from two experiments).

(G and H) Conditional genetic deletion of p38α in T cells via Cre-loxP in a murine T cell differentiation under Th17 (G) and Th1 (H) cell polarization (n = 6 per group, data pooled from two experiments).

*p < 0.05, **p < 0.01; ***p < 0.001. See also Figure S2.

effector T cells on day 14 p.i. with significantly decreased $CD4^+CD62L^{hi}$ cell frequency (and increased $CD62L^{lo}$ cell frequency, not shown) and increased $CD4^+CD44^{hi}$ cell frequency and $CD4^+CD25^{hi}$ cell frequency (Figure 4E). Splenocyte recall assays also revealed increased IFN-γ and IL-17A secretion on day 10 p.i. (Figures S4D and S4E). Via the same procedure, LA-rich diet increased T cell proliferation without additional stimulation; however, this effect was more significant in $CD4^+$ and $CD8^+$ T lymphocytes after MOG_{35-55}-specific recall (by 100%) or polyclonal activation by concanavalin A (by >300%, Figure 4F).

LA Exerts Effect on Th17 Cells via the Small Intestine

In order to elucidate the anatomic site of the observed in vivo actions of LA, we examined LA concentrations in the serum, blood cells, the complete duodenum, and duodenal mucosa after either LA-rich or control diet on day 10 p.i. We found that LA concentrations in the blood compartment (Figure 5A), mucosa, and duodenum (Figure 5B) were significantly increased after LA diet, with the highest concentrations in the blood compartment and an enrichment of LA in the duodenal mucosa versus the complete duodenum. More extensive analysis of FAs in these compartments also revealed an increase of MCFAs and LCFAs of various chain lengths, especially C14–C18 under an LA diet (Figures S5A–S5D). Given the enrichment of LA in the small intestine (SI) mucosa, we further scrutinized the gut. In a kinetic analysis of intraepithelial lymphocytes (IELs), lamina propria lymphocytes (LPLs), and Peyer's patches (PPs) in various gut locations, we found the most pronounced increase in IL-17A and IFN-γ on the protein level in LPLs of the SI 10 days p.i. (Figures 5C, 5D, S5E, and S5F). To monitor the dynamics of increased Th17 cell frequency under LA in EAE, we analyzed the SI more closely, quantifying Th17 cells in the SI LPLs between days 4 and 21 p.i. Ex vivo flow cytometry analysis of relative Th17 cell abundance in the SI LPLs on days 4, 7, 10, and 14 p.i. showed an initial increase of Th17 cells in SI LPLs, with a maximum at day 7 and a subsequent gradual reduction after day 10 (Figure 5E), coinciding with the onset of symptoms in EAE (Figure 4A). A cell transfer experiment on day 10 p.i. corroborated these data with an increased accumulation of MOG-activated, labeled T cells, specifically in the SI LPLs of LA-diet-fed mice (Figure 5F). Intestinal Treg cell frequencies were not affected (Figures S5G and S5H). The increase of Th17 cells was specific for MOG_{35-55} immunized mice; we did not observe any changes in Th17 cell frequency in naive control mice or mice 10 days p.i. with complete Freund's adjuvant (CFA) only (Figure S5I).

To further investigate whether metabolites of the gut microbiota are involved in LA's enhancing effect on Th17 cells, we added fecal filtrates from either LA- or control-diet mice to naive T cells under Th17-cell-polarizing conditions. The addition of fecal filtrates from LA-diet mice resulted in higher numbers of Th17 cells than from control diet (Figure 5G), arguing for the involvement of the local microbiome and their metabolic changes in the SI. Metabolite analyses revealed that not only were the longer-chain FAs increased under LA diet (Figures S5A–S5D), but levels of SCFAs and particularly PA were significantly decreased in the feces of LA-fed mice (Figure 5H), thus lending additional support for the crucial involvement of gut microbiota and metabolites in the effect of LA on Th17 cells.

We also performed a microbiome analysis of feces sampled on day 10 p.i. with MOG_{35-55} versus naive mice. Although EAE itself did not alter microbiome composition, the LA diet reduced Prevotellaceae and S24-7 families of the Bacteroidetes phylum as compared to controls (Figure 5I and Table S1).

Finally, for optimal investigation of LA-mediated microbial effects on intestinal Th17 cells in vivo, we employed the anti-CD3-specific antibody treatment model, which is characterized by an acute immune activation and a particular susceptibility of the SI to enhanced inflammation (Chatenoud and Bluestone, 2007; Esplugues et al., 2011). Usage of this model revealed a pronounced increase of Th17 cell frequency in SI IELs as compared to naive control mice (Figure S5J). In line with our data from the EAE model, we observed a further increase in IEL Th17 cell frequency under an LA-rich diet after anti-CD3 antibody injections (Figure S6K). This effect could be reproduced in vivo via oral transfer of feces from LA-diet-fed mice into germ-free (GF) recipients. These mice were found to have higher frequencies of Th17 cells in IELs as compared to control GF mice having received feces from mice under a control diet (Figure 5J). Further, gut microbiota were found to be necessary for the effect of LA on Th17 cell increase, as no Th17 cells were detectable in the SI after feeding only LA to control GF mice (Figure 5K).

In Vivo, PA-Mediated Treg Cell Regulatory Response Ameliorates CNS Autoimmunity

To evaluate whether the opposing effect of the C3 FA PA seen in vitro exerts an ameliorating effect on the course of EAE, we applied 150 mM PA (or water solvent) by daily oral gavage either (1) at the day of immunization (DI) or (2) at onset of disease (OD). In contrast to the LA-rich diet, application of PA revealed beneficial effects in EAE, but only in the preventive setting (Figure 6A). Ex vivo recall assays revealed a significant increase of the anti-inflammatory cytokine IL-10 in cells derived from PA-treated EAE, whereas, in contrast to LA-diet mice, no significant difference in IL-17A production was observed (Figure 6B). Phenotyping of SI LPLs on day 8 p.i. revealed increased $CD4^+CD25^+Foxp3^+$ Treg cell frequency in PA-treated EAE mice (Figure 6C). Analyses of the signature cytokines in different gut sub-compartments also showed increased mRNA levels of *Tgfb1*, *Il10*, and *Foxp3* in the distal parts of the SI in these mice (Figure 6D). To test whether orally delivered PA imprints a protective phenotype on Treg cells in vivo, we transferred Treg cells derived from PA-pre-treated (7 days) or untreated (5×10^5 $CD4^+CD25^+$ Treg cells; i.p.) mice into recipient mice concurrently with EAE induction; flow cytometry analysis of isolated cells confirmed the congruity of $Foxp3^+$ cell percentages in the transferred T cell preparations (69%–72% under both conditions). Treg cells derived from PA-pre-treated mice led to a marked improvement in the clinical course of the recipient EAE as compared to controls (Figure 6E). The improved clinical outcome in PA-DI-treated mice was reflected in the histopathological analyses of the spinal cord, with less inflammatory cell infiltration, less demyelination, and a higher degree of axonal preservation (Figure 6F).

DISCUSSION

Our data add FAs to the list of environmental triggers of T cell differentiation that might act as risk factors for Th1-cell- and/or

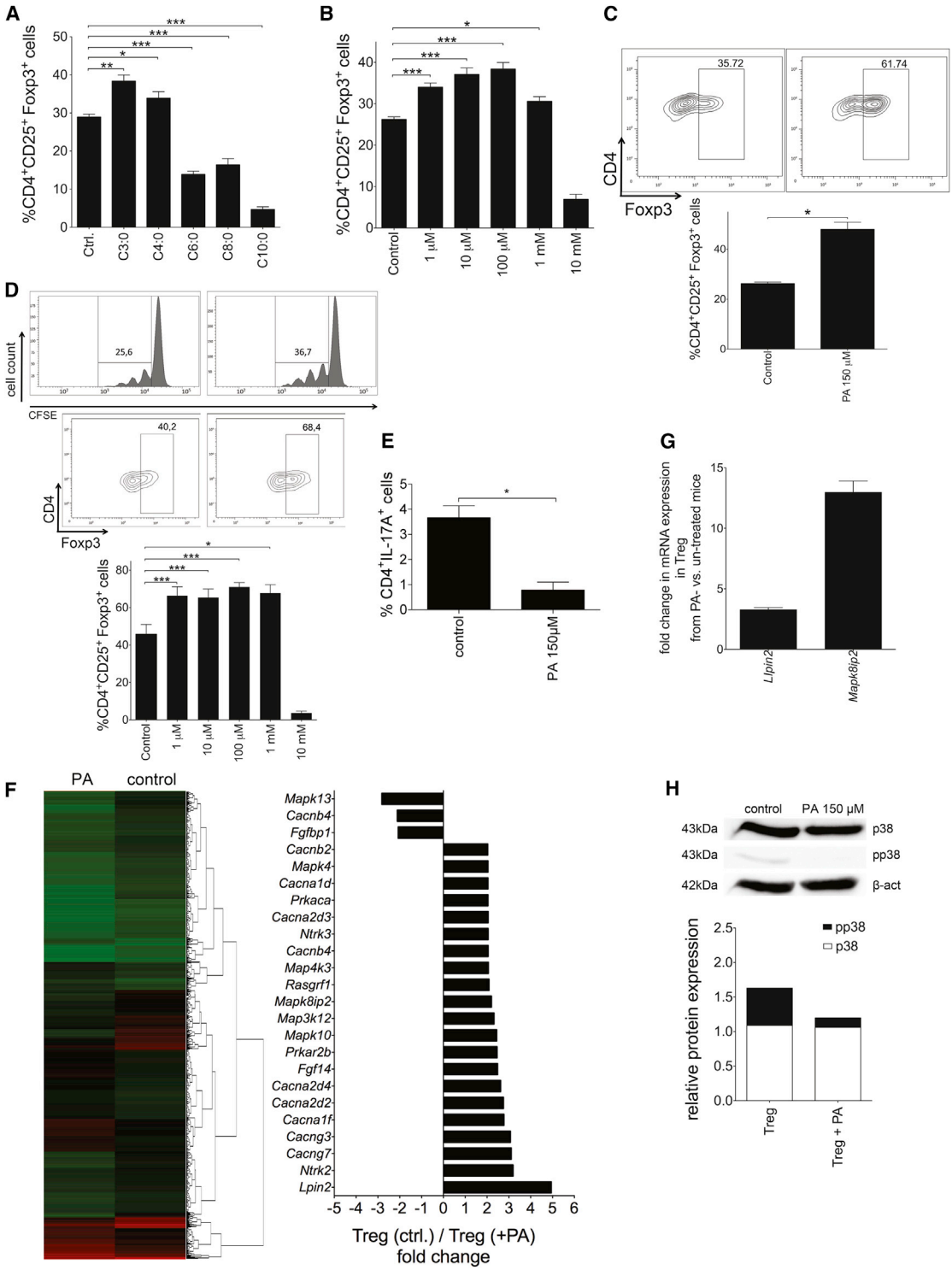

Figure 3. SCFAs Promote Polarization of Naive T Cells toward Treg Cells and Suppress the JNK1 and p38 Pathway

(A) Addition of FA derivatives to murine CD4$^+$ T cells under Treg cell polarizing conditions. C3:0 PA, C4:0 butyric acid, C6:0 caproic acid, C8:0 caprylic acid, C10:0 capric acid, C12:0 lauric acid (all FAs at 100 µM; n = 7).

(B) Addition of different PA concentrations to murine Treg cell differentiation (n = 8).

(C) Addition of PA to murine CD4$^+$ T cell differentiation culture under Treg cell polarizing conditions (n = 8).

(D) Addition of PA to human CD4$^+$ T cell proliferation and differentiation culture under Treg cell polarizing conditions (n = 5, one out of two experiments shown).

(E) Addition of PA to human CD4$^+$ T cell proliferation and differentiation culture under Th17 cell polarizing conditions (n = 5, one out of two experiments shown).

(legend continued on next page)

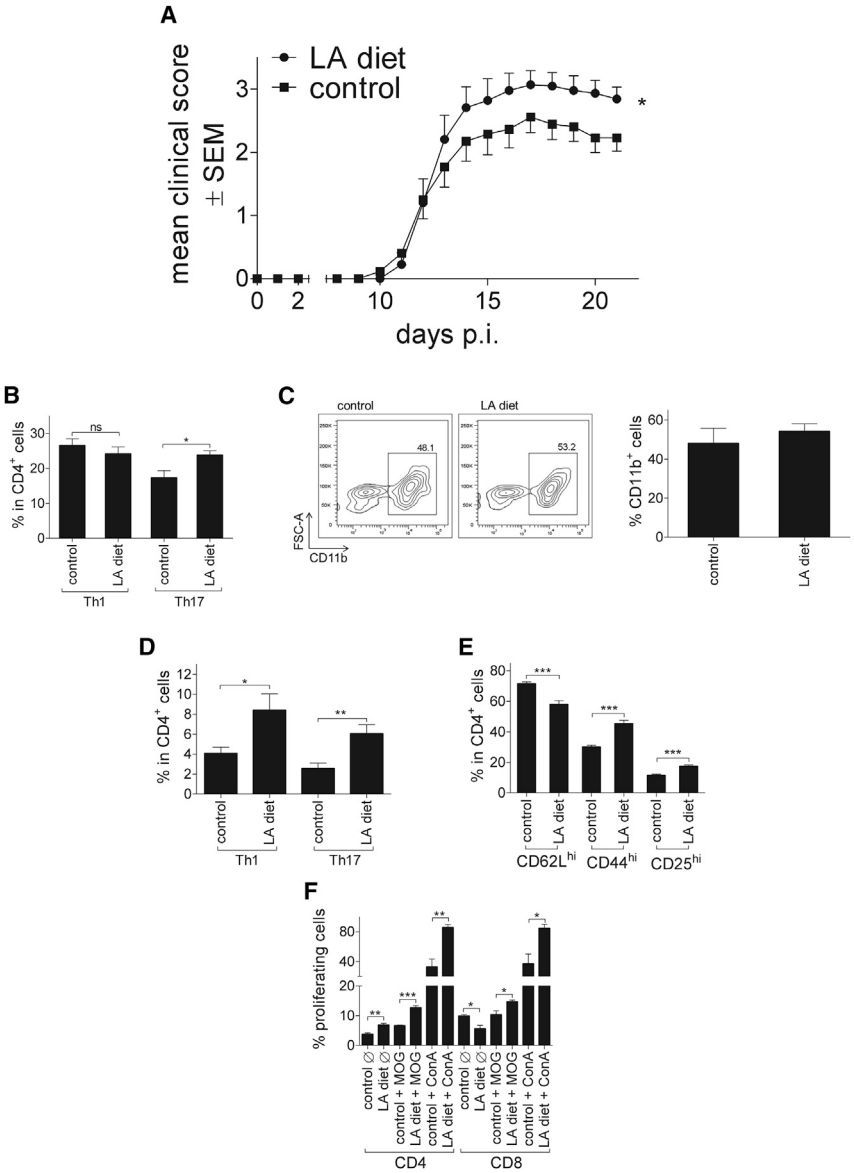

Figure 4. LA Exacerbates CNS Autoimmunity and Increases Th1 and Th17 Cells In Vivo

(A) Clinical course of MOG_{35-55} EAE. Mice were fed a LA-rich diet (n = 10) or control diet (n = 13) for 4 weeks prior to immunization. Data are shown on a 5-point score scale pooled from two experiments.

(B and C) Ex vivo flow cytometry analysis of (B) Th1 and Th17 cell frequencies and $CD11b^+$ cells (C) in the spinal cord under LA-rich versus control diet on day 14 of MOG_{35-55} EAE (n = 7 per group).

(D) Ex vivo flow cytometry analysis of Th1 and Th17 cell frequencies in the spleen on day 10 of MOG_{35-55} EAE (n = 7 versus 10 mice per group).

(E) Ex vivo flow cytometry analysis of $CD25^+$, $CD44^+$, or $CD62L^{hi}$ effector T cells from spleen on day 14 of MOG_{35-55} EAE under LA-rich versus control diet (n = 7 per group).

(F) Proliferation of $CD4^+$ and $CD8^+$ T cells after ex vivo recall with MOG_{35-55} (splenocytes harvested on day 14 p.i. of MOG_{35-55} EAE, n = 4 per group). Ø = none

ns = not significant, *p < 0.05, **p < 0.01; ***p < 0.001. See also Figure S4.

Th17-cell-mediated autoimmune diseases like MS (Kleinewietfeld and Hafler, 2014). Recent epidemiological studies reveal that lifestyle factors such as smoking, obesity, and salt intake might constitute a risk for MS (Hedström et al., 2011, 2014; Kleinewietfeld et al., 2013). Because such a diet is also typically rich in FAs, our present data offer important immunological and functional groundwork for epidemiological observations and identify saturated FAs as a new dietary, non-infectious trigger involved in intestinal T cell differentiation due to the interaction of gut-hosted microbiota and nutritional metabolites.

Here we show that, in autoimmune disease, FAs exert direct effects both on murine and human Th cells under polarizing conditions in vitro and in the context of antigen-specific T cell response in vivo. Treatment with SCFAs, PA most potently, enhanced differentiation and proliferation of $CD4^+CD25^+Foxp3^+$ Treg cells and ameliorated EAE disease course. In contrast, MCFAs or LCFAs such as LA or PALM enhanced Th1 and Th17 cell differentiation and contributed to a more severe course of EAE. The simultaneous increase of tracked Th17 cells in the spleen and CNS together support a model of differential segregation of antigen-specific T cells under an LA-rich diet. This hypothesis is further supported by the increased levels of LA found in the blood and mucosa compartments in mice having received an LA-rich diet. The increase of LA in both compartments might explain not only the systemic effect of LA on Th17 cell differentiation in vivo, but also the increased frequency of Th17 cells in the lamina propria during the initial antigen-specific immune response in EAE.

(F) Heat map analysis displaying differentially expressed genes (DEG) in the transcriptome analysis of Treg cell derived from PA pre-treated or previously untreated (control) mice (left). Right: a selection of 24 up- and downregulated genes.

(G) Validation of DEG detected by the transcriptome analysis via qRT-PCR showing upregulation of *Lpin-2* (lipin-2) and marked mRNA upregulation of *mapk8ip2* (JNK1 interacting protein2, JIP2) in Treg cells derived from mice pre-treated with PA as compared to Treg cells from untreated mice (from five independent preparations).

(H) Immunoblot analysis of p38 and phosphorylated p38 protein (pp38) in Treg cell differentiation assays with and without PA. β-actin (β-act) was used as loading control.

*p < 0.05, **p < 0.01, ***p < 0.001. See also Figure S3.

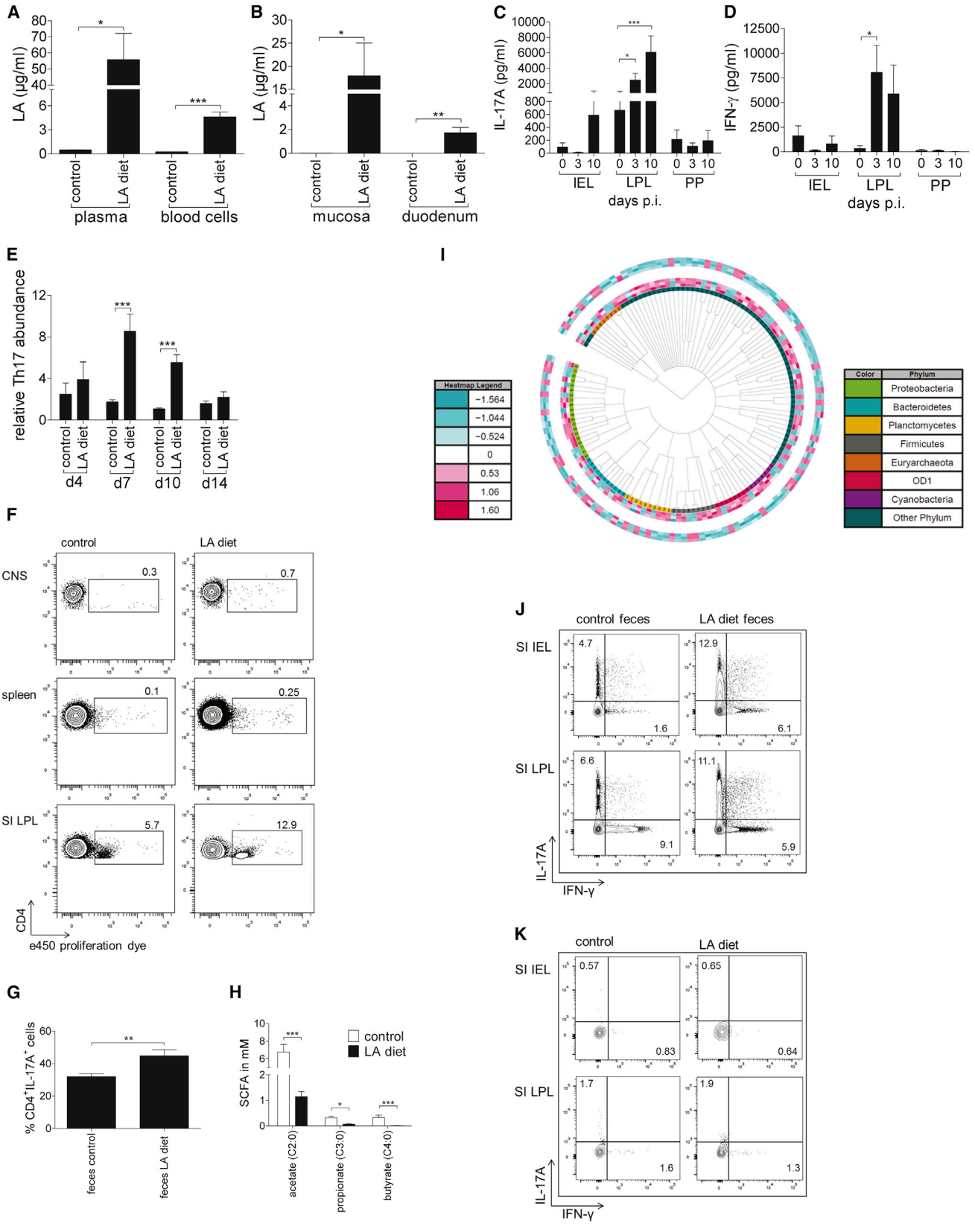

(legend on next page)

The proposed FA-receptor mediating the aforementioned effects remains to be identified. The presented divergent effects of saturated FAs on Th1 and Th17 versus Treg cells depended on the length of the carbon chain backbone, thus arguing for a pattern- or chain length-sensing receptor on T cells. Here, GPR109 might be a critical player, as has been recently shown for butyric acid (Singh et al., 2014), whereas receptors previously noted of importance, GPR41 and GPR43 (Kim et al., 2013), are not as relevant in our system. Given the plasticity of Th17 and Treg cells and their complex, divergent, intercellular signaling pathways during differentiation (for review see Kleinewietfeld and Hafler, 2014), it is likely that several mechanisms act in concert.

On both the gene expression and post-transcriptional levels (protein), members of the MAP kinase family, including p38 and JNK1, along with lipin-2 and their regulation of downstream pathways, are herein identified as crucial mediators of the effects of saturated FAs on T cells. Although both p38 and JNK1 have been shown to non-redundantly contribute to T cell death, differentiation, and proliferation (Rincón and Pedraza-Alva, 2003), p38-MAPK in particular is a well-known integrator of environmental stress and is involved in both T cell differentiation (Kleinewietfeld et al., 2013) and models of MS (Krementsov et al., 2014; Noubade et al., 2011). Because p38-MAPK plays a prominent role in T cell development and function (Alam et al., 2014), it can be argued that developmental changes due to the genetic knock-out of p38-MAPK lead to future alterations of T cell differentiation prior to the application of FAs. However, pharmacological blockage of this pathway after T cell development confirmed its specific involvement in FA effects on T cell differentiation. Indeed, the coupling of both the p38 and JNK MAP kinase pathways to T cell receptor signaling might allow for lineage-specific signals in T cell differentiation (Flavell et al., 1999). Additionally, our identification of lipin-2 signaling in the PA-induced generation of Treg cells adds to previous literature whereby it has been shown to counteract the pro-inflammatory effects of saturated FAs on macrophages (Valdearcos et al., 2012), yet it had not been previously described in the context of T cells.

In addition to the MAP kinase family members, transcription factor c-Maf and kinase SGK1, both of which have been shown to be critically involved in Th17 cell differentiation (Tanaka et al., 2014; Wu et al., 2013), were among the differentially expressed genes identified in LA-treated T cells under Th17-cell-polarizing conditions.

In the absence of antigen, the expansion of Th17 cells in the SI of anti-CD3-treated mice clearly increased under LA feeding. Despite its limitations, especially in the context of CNS autoimmunity, the ability of anti-CD3 to induce acute immune activation offers a valuable setup to shed further light on the distribution of auto-antigen-specific Th cells under an LA-rich diet (Esplugues et al., 2011). Indeed, our observation of an increased influx of Th17 cells into the SI, e.g., the lamina propria, of LA-fed mice during EAE, provides evidence for the involvement of the SI, including nutritional metabolites and microbiota of the gut, in systemic T cell immune responses prior to T cell CNS infiltration.

The shift of the gut microbiome toward decreased Prevotellaceae and Bacteroidetes after an LA-rich diet might partially explain the enhanced positive effect of fecal transplantations over diet manipulation. This concept is backed by the observed decrease in SCFAs in the gut under LA-rich diet along with recent reports implicating the pivotal role of Bacteroidetes in the fermentation of fiber-rich nutrition into SCFAs. Furthermore, a dysbiotic microbiome with lower proportions of Bacteroidetes has been associated with immune dysregulation and incidence of autoimmune disorders such as Crohn's disease and asthma (Macia et al., 2012; Trompette et al., 2014).

Of particular interest is the ability of PA to beneficially influence the generation of Treg cells (Arpaia et al., 2013). Our study posits PA as a potent compound with the capacity to restrain CNS autoimmunity via restoration of the altered Treg cell:effector T cell balance, which is disturbed in MS patients (Viglietta et al., 2004). So far, influencing MS via direct Treg cell manipulations, e.g., via superagonistic anti-CD28 antibodies, has been considered worthwhile (Beyersdorf et al., 2005) but not practically feasible outside of controlled experimental conditions (Hünig, 2012). In fact, PA is a common environmental compound that was traditionally part of many preservatives and is already ingested by many people at lower concentrations (Cummings et al., 1987). Given this wide range in everyday practice and

Figure 5. LA Exerts Effect on Th17 Cells via the Small Intestine

(A and B) Quantification of LA in plasma, blood cells (A), duodenal mucosa, and whole SI (B) of mice on a control or LA diet on day 10 p.i. (n = 4 per group).

(C and D) Analysis of IL-17A (C) and IFN-γ (D) production in anti-CD3 and anti-CD28 stimulated cultured IELs, LPLs, and PPs from the SI on day 0, 3, and 10 of MOG_{35-55} EAE by ELISA (n = 6 per group for day 0 and n = 4 per group for day 3 and 10 p.i., data pooled from two different experiments).

(E) Ex vivo flow cytometry analysis of relative Th17 cell abundance in SI LPLs on days 4, 7, 10, and 14 p.i. (n = 4–8 per group).

(F) Cell tracking experiment of e450-labeled splenocytes in CNS, spleen, and SI of LA and control diet mice. Single cell suspensions were analyzed by flow cytometry for $CD4^+e450^+$ cells. Representative contour plots are shown (n = 4 per group).

(G) Addition of fecal filtrates from either LA or control diet mice to murine $CD4^+$ T cell differentiation culture under Th17 cell polarizing conditions (n = 3, one out of two representative experiments shown).

(H) Quantification of SCFAs in feces of mice on a control or LA diet on day 10 p.i. (n = 5 per group).

(I) Three comparing samples from mice on an LA-rich diet (inner rings) versus samples from mice on a control diet (outer rings). Feces were sampled on day 10 p.i. (n = 3 per group) and compared to samples from the same mice before induction of EAE (n = 3 per group). From the 803 operational taxonomic units present in the study, 254 within 117 families were significantly different in one of the comparison groups. 22 families contained operational taxonomic units with both higher and lower abundance scores in the samples from mice under an LA-rich diet versus controls. An idealized tree is computed using taxonomic classifications. The color saturation indicates z-score (defined as the difference between sample abundance and mean abundance, divided by the standard variation), which represents the sample difference from the overall mean abundance. Dark blue indicates the OTU has low abundance relatively to other samples (z-score of −1.56); white indicates no difference from the mean; dark red indicates high abundance (z-score of 1.60).

(J and K) Ex vivo flow cytometry analysis of Th1 (J) and Th17 (K) cell frequencies in SI IELs and LPLs after anti-CD3 antibody injection and oral transfer of feces from LA-diet-fed mice into germ-free (GF) recipients as compared to control GF mice with transfer of feces from donor mice under a control diet. A representative contour plot is shown.

*$p < 0.05$, ***$p < 0.001$. See also Figure S5.

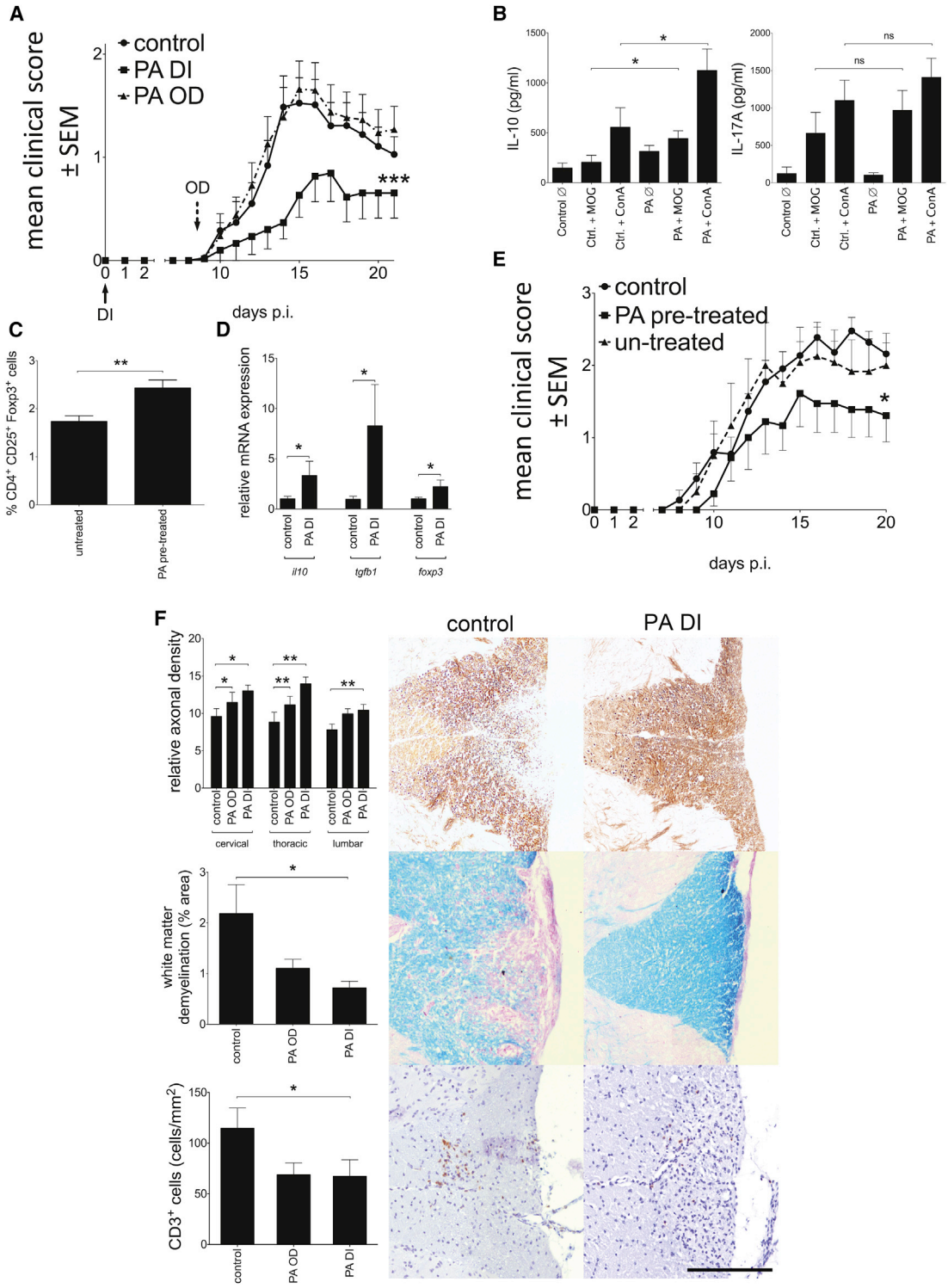

Figure 6. PA Ameliorates CNS Autoimmunity via Induction of Treg Cells in the Small Intestine

(A) Clinical course of MOG_{35-55} EAE. Mice received daily PA starting either at the day of immunization (DI, n = 15), at onset of disease (OD, n = 25), or the solvent water (controls, n = 29) via oral gavage in addition to the normal diet. Data are shown on a 5-point score scale pooled from three experiments.

(B) Cytokine measurement in cultures after ex vivo recall with MOG_{35-55} (splenocytes harvested on day 8 p.i. of MOG_{35-55} EAE, n = 8 versus 9 per group).

(C) Flow cytometry analysis of cells isolated from the LPLs of EAE either treated with PA (n = 5) or with water (untreated, n = 5) showing higher amount of Treg cells in PA-treated mice.

(D) Gene expression analyses of *tgfβ1*, *il10*, and *foxp3* in the SI LPLs of either PA (PA DI) or water (control) (triplicates, data pooled from seven to ten preparations).

(legend continued on next page)

growing evidence for the lasting dietary effect on microbiome composition (Cotillard et al., 2013), a rapid translation of PA therapy from pre-clinical studies to clinical trials in MS patients seems reasonable.

In sum, this study identifies dietary saturated FAs as crucial modulators in the gut, shifting Th1 and Th17 versus Treg cell balance in autoimmune neuroinflammation. We propose a dual mechanism of action for LA, comprising (1) increased Th17 and Th1 cell polarization and proliferation as a systemic effect and (2) enhanced sequestration of Th17 cells in the gut in the context of immune activation. Further studies in humans to explore the supplementary therapeutic potential of enriched diets are highly warranted.

EXPERIMENTAL PROCEDURES

EAE and Diet

For experiments under LA-rich diet, mice received a chow containing 30.9% crude fat rich in the MCFA C12:0 (lauric acid, 13.47%), and mice on a control diet were fed a chow with 4.2% crude fat. Mice were adapted to high-fat chow 4 weeks before EAE induction. For EAE under PA, either 200 μl PA (150 mM) or solvent (water) were applied daily via oral gavage in addition to normal diet with 3.3% crude fat, at either day of immunization (DI) or onset of disease (OD). For transfer experiments, mice received either PA or water via oral gavage in addition to normal diet for 7 days before gut Treg cells were isolated and injected into EAE at DI.

For EAE, 8- to 11-week-old mice were anesthetized and subcutaneously injected with 200 μg MOG_{35-55} and 200 μg CFA. Pertussis toxin (200 ng/mouse) was applied i.p. on days 0 and 2 p.i. Daily clinical evaluation was performed via a 5-point scale. All experiments were in accordance with the German laws for animal protection and were approved by the local ethic committees (Erlangen AZ 54-2532.1-56/12; Bochum AZ 84-02.04.2014.A104). For details and providers of materials used, see Supplemental Information.

In Vivo T Cell Stimulation

Mice on LA-rich or control diet were i.p. injected with anti-CD3 (20 μg, 145-2C11, BD PharMingen) or with PBS alone or CFA in PBS and sacrificed after 3 days.

Murine T Cell Culture and Differentiation

Splenic T cells were isolated by MACS, collected, and re-suspended in MACS buffer at 3 × 10^7 cells/ml. For Th17 cell differentiation, sorted naive T cells ($CD4^+CD62L^+CD44^{lo}CD25^-$) were stimulated by 2 μg/ml anti-CD3 and 2 μg/ml anti-CD28 in the presence of IL-6 (40 ng/ml) and rhTGF-β1 (1 ng/ml) for 4 days. For Th1 cell differentiation, naive $CD4^+$ T cells were cultured for 96 hr with anti-CD3, anti-CD28, IL-12 (20 ng/ml), and anti-IL-4 (10 mg/ml). For Treg cell differentiation, anti-CD3, anti-CD28, and rhTGF-β1 (1 ng/ml) were added to culture media. To determine the influence of FAs on T cell differentiation and proliferation, cells were cultured with and without 250 μM or 500 μM LA, 150 μM PA, or other FA derivatives (C4:0, C6:0, C8:0, C10:0) at concentrations ranging from 1 μM to 10 mM. In some experiments, sterile fecal filtrate from LA- or control-diet mice was added to the cultures: 200 mg feces were re-suspended in 1 ml ReMed and centrifuged, with 50 μl of sterile filtered supernatant added to T cell differentiation assays. For intracellular stainings (flow cytometry), cells were stimulated for 4 hr with ionomycin (1 μM) and PMA (50 ng/ml) in the presence of monensin (2 μM) and stained for CD4, intracellular IL-17A, and IFN-γ. Treg cells were stained by using the $FoxP3^+$ Treg cell staining kit according to the manufacturers' protocol. For details and providers of materials used, see Supplemental Information.

Human T Cell Differentiation

PBMCs from whole blood of healthy volunteers were separated by Ficoll-Paque PLUS gradient centrifugation and naive ($CD45RA^-CD45RO^+CD25^-CD127^+$) $CD4^+$ T cells were subsequently isolated by fluorescence-activated cell sorting on MoFlo. Naive T cells were cultured (5.3 × 10^4 cells) in serum-free X-VIVO15 medium or serum-free LGM 3 medium for 5 to 7 days and stimulated with anti-CD3 (10 μg/ml) and anti-CD28 (1 μg/ml). For Th1 cell differentiation, naive T cells were cultured with IL-12 (10 ng/ml) and anti-IL-4 (10 μg/ml); IL-1β (12.5 ng/ml), IL-6 (25 ng/ml), IL-21, IL-23 (25 ng/ml), and rhTGF-β1 (10 ng/ml) for Th17 cells; rh-TGF-β1 (5 ng/ml) for Treg cells. For investigating the influence of FAs on T cell differentiation, PALM and LA were added to the cultures. All cells were analyzed via flow cytometry analysis. For details and providers, see Supplemental Information.

In Vitro MOG Restimulation Assay

Splenocytes from EAE mice were obtained on day 10 p.i. and seeded at a density of 3 × 10^6 cells/ml in Re-medium. MOG_{35-55} (1, 20, 100 μg/ml) and ConA (1.25 μg/ml) were added for stimulation, and cells were cultured 48 hr. Supernatants were harvested and analyzed for cytokines (ELISA). To monitor proliferation, cells were labeled with fixable proliferation dye (eBioscience) according to the manufacturer's protocol.

Co-culture Assay with Dendritic Cells

Bone marrow cells were isolated from femur and tibia, re-suspended in R10 medium containing GM-CSF (5 ng/ml) and IL-4 (5 ng/ml), and cultured for 10 days with/without 250 μM LA. Medium was changed on days 3 and 6, and cells were matured on day 8 with 1 μg/ml LPS (Sigma-Aldrich) and 20 μg/ml MOG_{35-55}. For the co-culture assay, mature DCs were seeded with MOG-specific transgenic naive T cells in a ratio of 1:6 with/without 250 μM LA. After Th17 cell differentiation, Th17 cell frequencies were analyzed 96 hr later by intracellular staining via flow cytometry analysis.

Cell Tracking Experiment

Splenocytes from EAE mice were obtained on day 10 p.i., labeled with fixable e450 proliferation dye (eBioscience), and intravenously transferred into mice on a LA or control diet on day 10 p.i. (25 × 10^6 cells/mouse). Spleens, CNS, and SI of recipient mice were scrutinized on day 4 post cell transfer and analyzed by flow cytometry for $CD4^+e450^+$ cells.

Free Fatty Acid Quantification

Total fatty acid concentrations in plasma, whole blood cells, and duodenum of mice on a LA or control diet were analyzed on day 10 p.i. via gas chromatography (GC) as described (Ostermann et al., 2014). In brief, lipids were extracted with MTBE/MeOH and derivatized with methanolic hydrochloric acid, and the resulting FAME were quantified by GC with flame ionization detection. For details of SCFAs analyses in feces, see Supplemental Information.

Microbiome Analysis

Frozen DNA isolated from mice fecal sample with total masses ranging from 1.3 to 38.7 ng were stored at −20°C. The bacterial 16S rRNA genes were amplified (35 cycles) using the degenerate forward primer 5′-AGRGTTTGAT CMTGGCTCAG-3′ and the non-degenerate reverse primer 5′-GGTTACCTTG TTACGACTT-3′. Each amplified product was concentrated via solid-phase reversible immobilization and quantified by electrophoresis using an Agilent

(E) Clinical course of Treg cells transferred into MOG_{35-55} EAE. EAE mice received either 5 × 10^5 $CD4^+CD25^+$ Treg cells from PA pre-treated donor animals (n = 6) or from previously untreated mice (n = 9), or received PBS (control, n = 11) on the day of immunization. Data are shown on a 5-point score scale pooled from two experiments.

(F) Histological analyses of axons, demyelination, and cellular infiltration the spinal cord of PA-DI-treated (n = 9 sections from 7 independently analyzed mice) and PA-OD-treated (n = 9 sections from 5 independently analyzed mice) EAE as compared to the controls (n = 9 sections from 5 independently analyzed mice). Perfusion and spinal cord removal on day 20–22 p.i. of MOG_{35-55} EAE; scale bar represents 100 μm.

*p < 0.05, **p < 0.01, ***p < 0.001.

2100 Bioanalyzer (Agilent). PhyloChip Control Mix was added to each amplified product. Bacterial 16S rRNA gene amplicons were fragmented, biotin labeled, and hybridized to the PhyloChip Array (Affymetrix), version G3. PhyloChip arrays were washed, stained, and scanned with a GeneArray scanner (Affymetrix). Each scan was captured with standard Affymetrix software (GeneChip Microarray Analysis Suite, Affymetrix). Samples were processed in a Good Laboratory Practices compliant service laboratory running quality-management systems for sample, data tracking, and data analysis (Second Genome).

Fecal Transplant

200 mg feces from mice on LA or control diet were collected in a sterile manner on the day of fecal transfer and re-suspended in 1 ml sterile filtered autoclaved tap water and adjusted to a final volume of 200 mg feces/ml, vortexed, and centrifuged. Each recipient mouse received 200 μl of fecal supernatant by oral gavage on 3 consecutive days before αCD3 injection (20 μg/mouse, 145-2C11, BD PharMingen) after 3 weeks of housing in sterile cages with sterile autoclaved water and autoclaved food.

Transcriptome Analysis

Total RNA was isolated from corresponding cells using the RNeasy Mini Kit (QIAGEN) with prior peqGOLD TriFast (Peqlab) treatment. cDNA was generated with Ambion WT Expression Kit (Life Technologies). Subsequently, Affymetrix GeneChip Mouse Gene ST Arrays were processed by the manufacturer's protocol. Data were processed with the Affymetrix Expression Console and Transcriptome Analysis Console v.2.0 (TAC) software, and candidate genes were selected rationally under consideration of both gene functions found in literature (NCBI and GeneCards) and integrative pathway analyses by Ingenuity Pathway Analysis (IPA, QIAGEN).

Statistical Analysis

Statistical analysis was performed with GraphPad Prism (GraphPad Software). All in vitro and ex vivo data were analyzed by one-way ANOVA followed by Tukey's post test, unpaired t test, or Wilcoxon rank sum test after checking for normal distribution (unless indicated otherwise in the legends), EAE data by Kruskal-Wallis, and Mann-Whitney U test. Data are presented as mean ± SEM; *$p < 0.05$, **$p < 0.01$, or ***$p < 0.001$ were considered to be statistically significant.

SUPPLEMENTAL INFORMATION

Supplemental Information includes five figures, one table, and Supplemental Experimental Procedures (including isolation of CNS-infiltrating lymphocytes, splenic lymphocytes, immune cell analysis in the gut, immunohistochemistry and tissue staining, flow cytometry analysis, cytokine detection, real-time PCR, and immunoblotting) and can be found with this article online at http://dx.doi.org/10.1016/j.immuni.2015.09.007.

AUTHOR CONTRIBUTIONS

A. Haghikia and S.J. planned and performed experiments and analyses. A. Haghikia and R.A.L. designed the study and planned as well as supervised the research. A. Haghikia, S.J., and R.A.L. wrote the manuscript. R.G. designed the study, supervised the research, and edited the manuscript. A.D., J.B., A.M., A.W., A. Hammer, D.-H.L., N.W., A.B., A.I.O., D.A.A., D.A.G., S.K., J.T., and S.D. performed experiments. N.H.S., M.K., and D.N.M. analyzed the data and edited the manuscript.

ACKNOWLEDGMENTS

We wish to thank S. Seubert, K. Bitterer, and X. Pedreiturria for expert technical assistance. The authors also thank Megan Massa (B.A. Neuroscience) for editing the language of the manuscript. Cell sorting was supported by the FACS Core Unit, Nikolaus-Fiebiger-Center, Friedrich-Alexander-University Erlangen, Germany. R.A.L. holds an endowed professorship supported by the Novartis Foundation. This study was supported by the Deutsche Forschungsgesellschaft (DFG) grant CRC128/Z2 (to R.G.).

Received: November 13, 2014
Revised: April 7, 2015
Accepted: July 21, 2015
Published: October 20, 2015

REFERENCES

Alam, M.S., Gaida, M.M., Ogawa, Y., Kolios, A.G., Lasitschka, F., and Ashwell, J.D. (2014). Counter-regulation of T cell effector function by differentially activated p38. J. Exp. Med. *211*, 1257–1270.

Arpaia, N., Campbell, C., Fan, X., Dikiy, S., van der Veeken, J., deRoos, P., Liu, H., Cross, J.R., Pfeffer, K., Coffer, P.J., and Rudensky, A.Y. (2013). Metabolites produced by commensal bacteria promote peripheral regulatory T-cell generation. Nature *504*, 451–455.

Berer, K., Mues, M., Koutrolos, M., Rasbi, Z.A., Boziki, M., Johner, C., Wekerle, H., and Krishnamoorthy, G. (2011). Commensal microbiota and myelin autoantigen cooperate to trigger autoimmune demyelination. Nature *479*, 538–541.

Beyersdorf, N., Gaupp, S., Balbach, K., Schmidt, J., Toyka, K.V., Lin, C.H., Hanke, T., Hünig, T., Kerkau, T., and Gold, R. (2005). Selective targeting of regulatory T cells with CD28 superagonists allows effective therapy of experimental autoimmune encephalomyelitis. J. Exp. Med. *202*, 445–455.

Bhargava, P., and Lee, C.H. (2012). Role and function of macrophages in the metabolic syndrome. Biochem. J. *442*, 253–262.

Brown, E.M., Sadarangani, M., and Finlay, B.B. (2013). The role of the immune system in governing host-microbe interactions in the intestine. Nat. Immunol. *14*, 660–667.

Chatenoud, L., and Bluestone, J.A. (2007). CD3-specific antibodies: a portal to the treatment of autoimmunity. Nat. Rev. Immunol. *7*, 622–632.

Clemente, J.C., Ursell, L.K., Parfrey, L.W., and Knight, R. (2012). The impact of the gut microbiota on human health: an integrative view. Cell *148*, 1258–1270.

Cotillard, A., Kennedy, S.P., Kong, L.C., Prifti, E., Pons, N., Le Chatelier, E., Almeida, M., Quinquis, B., Levenez, F., Galleron, N., et al.; ANR MicroObes consortium (2013). Dietary intervention impact on gut microbial gene richness. Nature *500*, 585–588.

Cummings, J.H., Pomare, E.W., Branch, W.J., Naylor, C.P., and Macfarlane, G.T. (1987). Short chain fatty acids in human large intestine, portal, hepatic and venous blood. Gut *28*, 1221–1227.

Esplugues, E., Huber, S., Gagliani, N., Hauser, A.E., Town, T., Wan, Y.Y., O'Connor, W., Jr., Rongvaux, A., Van Rooijen, N., Haberman, A.M., et al. (2011). Control of TH17 cells occurs in the small intestine. Nature *475*, 514–518.

Flavell, R.A., Li, B., Dong, C., Lu, H.T., Yang, D.D., Enslen, H., Tournier, C., Whitmarsh, A., Wysk, M., Conze, D., et al. (1999). Molecular basis of T-cell differentiation. Cold Spring Harb. Symp. Quant. Biol. *64*, 563–571.

Furusawa, Y., Obata, Y., Fukuda, S., Endo, T.A., Nakato, G., Takahashi, D., Nakanishi, Y., Uetake, C., Kato, K., Kato, T., et al. (2013). Commensal microbe-derived butyrate induces the differentiation of colonic regulatory T cells. Nature *504*, 446–450.

Haghikia, A., Hohlfeld, R., Gold, R., and Fugger, L. (2013). Therapies for multiple sclerosis: translational achievements and outstanding needs. Trends Mol. Med. *19*, 309–319.

Hedström, A.K., Sundqvist, E., Bäärnhielm, M., Nordin, N., Hillert, J., Kockum, I., Olsson, T., and Alfredsson, L. (2011). Smoking and two human leukocyte antigen genes interact to increase the risk for multiple sclerosis. Brain *134*, 653–664.

Hedström, A.K., Lima Bomfim, I., Barcellos, L., Gianfrancesco, M., Schaefer, C., Kockum, I., Olsson, T., and Alfredsson, L. (2014). Interaction between adolescent obesity and HLA risk genes in the etiology of multiple sclerosis. Neurology *82*, 865–872.

Hünig, T. (2012). The storm has cleared: lessons from the CD28 superagonist TGN1412 trial. Nat. Rev. Immunol. *12*, 317–318.

Kim, M.H., Kang, S.G., Park, J.H., Yanagisawa, M., and Kim, C.H. (2013). Short-chain fatty acids activate GPR41 and GPR43 on intestinal epithelial cells

to promote inflammatory responses in mice. Gastroenterology *145*, 396–406.e1, 10.

Kleinewietfeld, M., and Hafler, D.A. (2014). Regulatory T cells in autoimmune neuroinflammation. Immunol. Rev. *259*, 231–244.

Kleinewietfeld, M., Manzel, A., Titze, J., Kvakan, H., Yosef, N., Linker, R.A., Muller, D.N., and Hafler, D.A. (2013). Sodium chloride drives autoimmune disease by the induction of pathogenic TH17 cells. Nature *496*, 518–522.

Krementsov, D.N., Noubade, R., Dragon, J.A., Otsu, K., Rincon, M., and Teuscher, C. (2014). Sex-specific control of central nervous system autoimmunity by p38 mitogen-activated protein kinase signaling in myeloid cells. Ann. Neurol. *75*, 50–66.

Lozupone, C.A., Stombaugh, J.I., Gordon, J.I., Jansson, J.K., and Knight, R. (2012). Diversity, stability and resilience of the human gut microbiota. Nature *489*, 220–230.

Macia, L., Thorburn, A.N., Binge, L.C., Marino, E., Rogers, K.E., Maslowski, K.M., Vieira, A.T., Kranich, J., and Mackay, C.R. (2012). Microbial influences on epithelial integrity and immune function as a basis for inflammatory diseases. Immunol. Rev. *245*, 164–176.

Noubade, R., Krementsov, D.N., Del Rio, R., Thornton, T., Nagaleekar, V., Saligrama, N., Spitzack, A., Spach, K., Sabio, G., Davis, R.J., et al. (2011). Activation of p38 MAPK in CD4 T cells controls IL-17 production and autoimmune encephalomyelitis. Blood *118*, 3290–3300.

Ostermann, A.I., Müller, M., Willenberg, I., and Schebb, N.H. (2014). Determining the fatty acid composition in plasma and tissues as fatty acid methyl esters using gas chromatography – a comparison of different derivatization and extraction procedures. Prostaglandins Leukot. Essent. Fatty Acids *91*, 235–241.

Qin, J., Li, Y., Cai, Z., Li, S., Zhu, J., Zhang, F., Liang, S., Zhang, W., Guan, Y., Shen, D., et al. (2012). A metagenome-wide association study of gut microbiota in type 2 diabetes. Nature *490*, 55–60.

Rincón, M., and Pedraza-Alva, G. (2003). JNK and p38 MAP kinases in CD4+ and CD8+ T cells. Immunol. Rev. *192*, 131–142.

Singh, N., Gurav, A., Sivaprakasam, S., Brady, E., Padia, R., Shi, H., Thangaraju, M., Prasad, P.D., Manicassamy, S., Munn, D.H., et al. (2014). Activation of Gpr109a, receptor for niacin and the commensal metabolite butyrate, suppresses colonic inflammation and carcinogenesis. Immunity *40*, 128–139.

Smith, P.M., Howitt, M.R., Panikov, N., Michaud, M., Gallini, C.A., Bohlooly-Y, M., Glickman, J.N., and Garrett, W.S. (2013). The microbial metabolites, short-chain fatty acids, regulate colonic Treg cell homeostasis. Science *341*, 569–573.

Tanaka, S., Suto, A., Iwamoto, T., Kashiwakuma, D., Kagami, S., Suzuki, K., Takatori, H., Tamachi, T., Hirose, K., Onodera, A., et al. (2014). Sox5 and c-Maf cooperatively induce Th17 cell differentiation via RORγt induction as downstream targets of Stat3. J. Exp. Med. *211*, 1857–1874.

Trompette, A., Gollwitzer, E.S., Yadava, K., Sichelstiel, A.K., Sprenger, N., Ngom-Bru, C., Blanchard, C., Junt, T., Nicod, L.P., Harris, N.L., and Marsland, B.J. (2014). Gut microbiota metabolism of dietary fiber influences allergic airway disease and hematopoiesis. Nat. Med. *20*, 159–166.

Valdearcos, M., Esquinas, E., Meana, C., Peña, L., Gil-de-Gómez, L., Balsinde, J., and Balboa, M.A. (2012). Lipin-2 reduces proinflammatory signaling induced by saturated fatty acids in macrophages. J. Biol. Chem. *287*, 10894–10904.

Viglietta, V., Baecher-Allan, C., Weiner, H.L., and Hafler, D.A. (2004). Loss of functional suppression by CD4+CD25+ regulatory T cells in patients with multiple sclerosis. J. Exp. Med. *199*, 971–979.

Wu, C., Yosef, N., Thalhamer, T., Zhu, C., Xiao, S., Kishi, Y., Regev, A., and Kuchroo, V.K. (2013). Induction of pathogenic TH17 cells by inducible salt-sensing kinase SGK1. Nature *496*, 513–517.

Immunity

Supplemental Information

Dietary Fatty Acids Directly Impact Central Nervous System Autoimmunity via the Small Intestine

Aiden Haghikia, Stefanie Jörg, Alexander Duscha, Johannes Berg, Arndt Manzel, Anne Waschbisch, Anna Hammer, De-Hyung Lee, Caroline May, Nicola Wilck, Andras Balogh, Annika I. Ostermann, Nils-Helge Schebb, Denis A. Akkad, Diana A. Grohme, Markus Kleinewietfeld, Stefan Kempa, Jan Thöne, Seray Demir, Dominik N. Müller, Ralf Gold, and Ralf A. Linker

Supplemental Figures

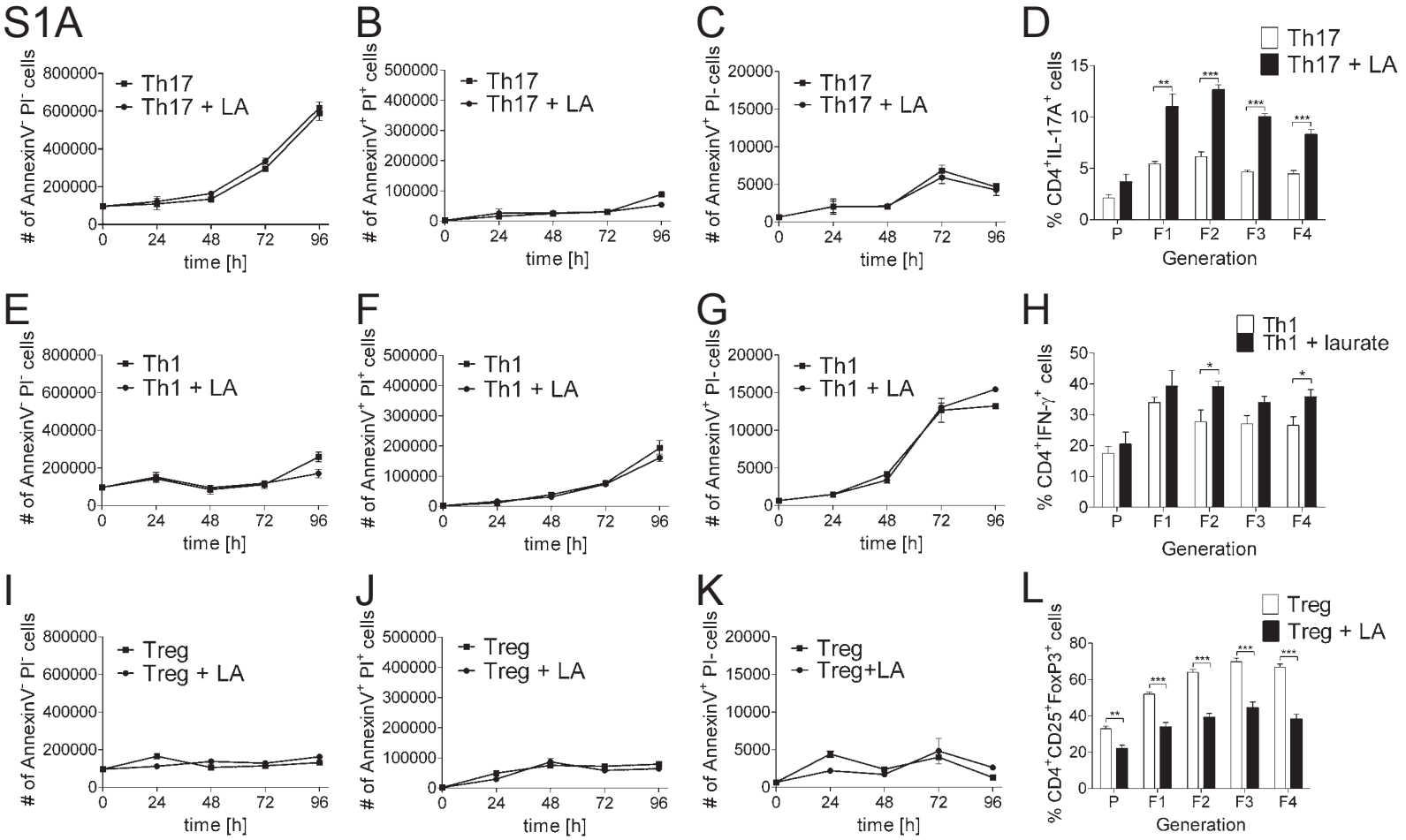

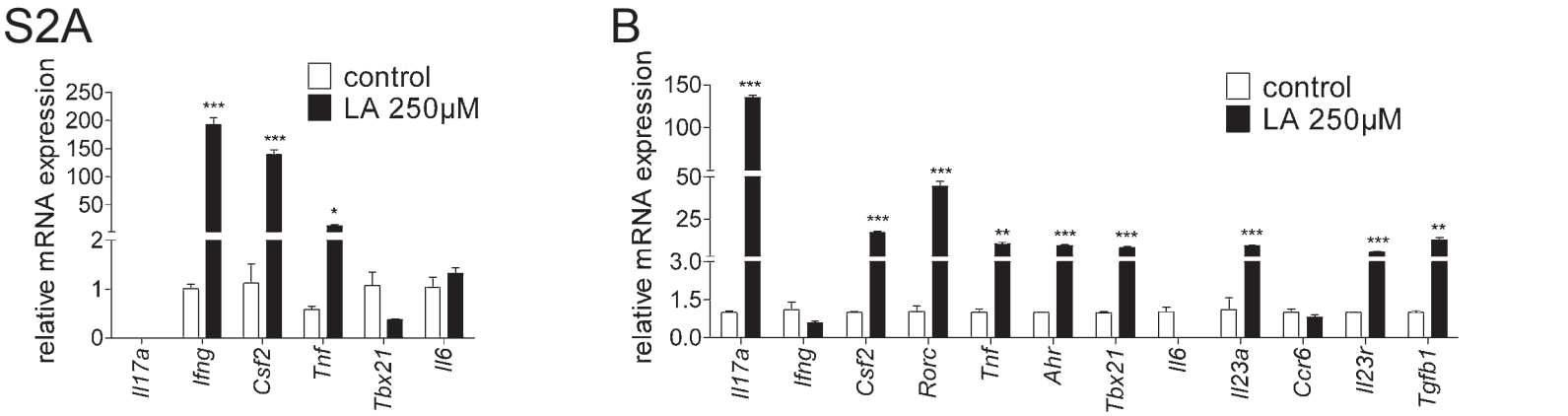

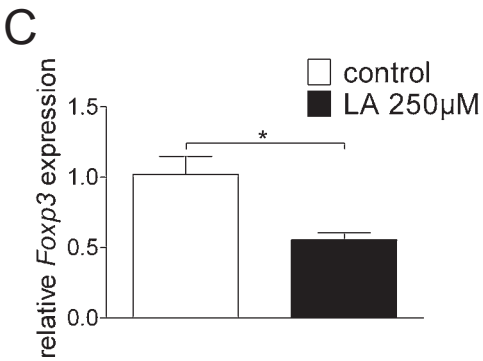

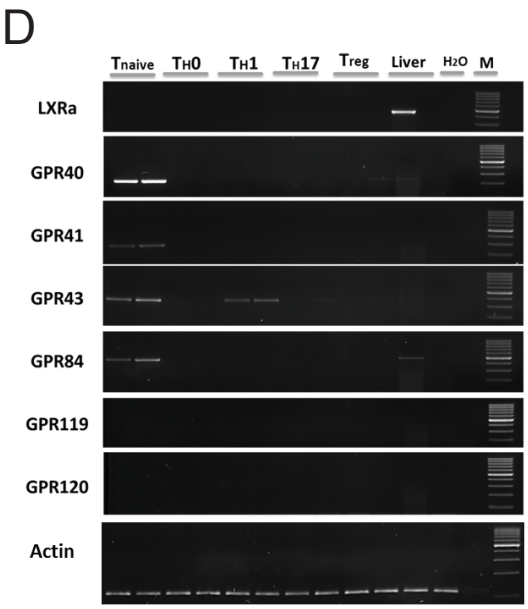

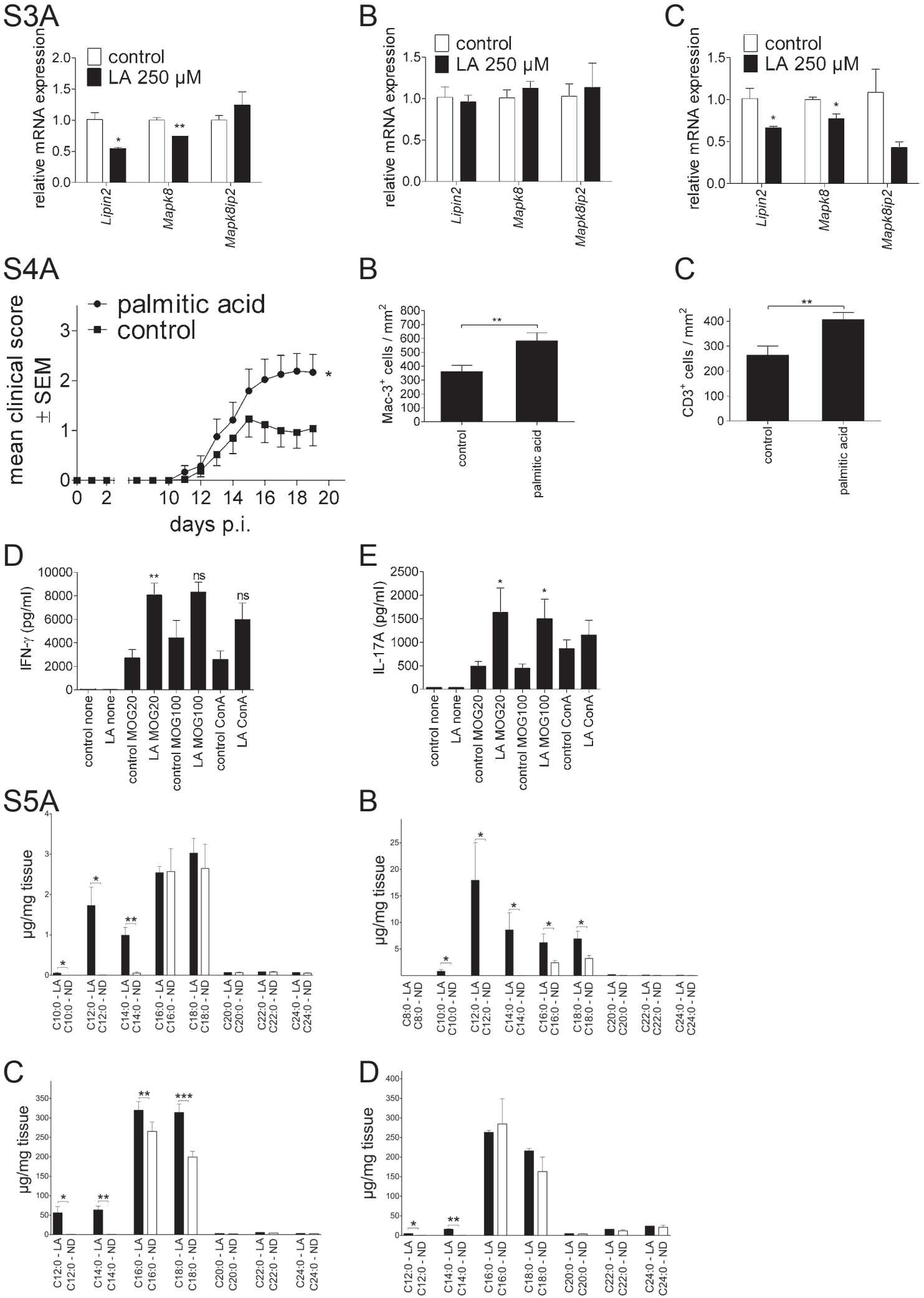
S3A
control
LA 250 µM
relative mRNA expression
Lipin2
Mapk8
Mapk8ip2
B
C
S4A
palmitic acid
control
mean clinical score ± SEM
days p.i.
Mac-3+ cells / mm2
CD3+ cells / mm2
D
IFN-γ (pg/ml)
E
IL-17A (pg/ml)
control none
LA none
control MOG20
LA MOG20
control MOG100
LA MOG100
control ConA
LA ConA
S5A
µg/mg tissue
C8:0 - LA
C8:0 - ND
C10:0 - LA
C10:0 - ND
C12:0 - LA
C12:0 - ND
C14:0 - LA
C14:0 - ND
C16:0 - LA
C16:0 - ND
C18:0 - LA
C18:0 - ND
C20:0 - LA
C20:0 - ND
C22:0 - LA
C22:0 - ND
C24:0 - LA
C24:0 - ND

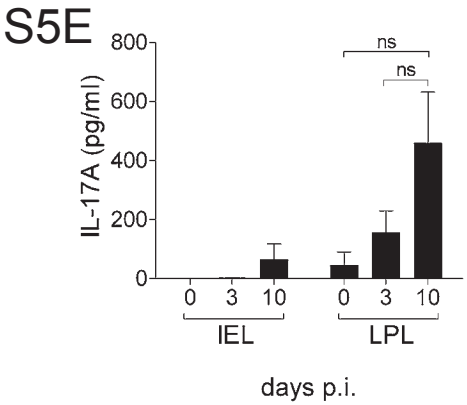
S5E
IL-17A (pg/ml)
800
600
400
200
0
ns
ns
0 3 10 0 3 10
IEL
LPL
days p.i.

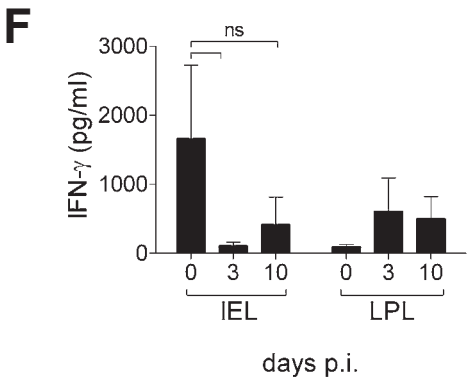
F
IFN-γ (pg/ml)
3000
2000
1000
0
ns
0 3 10 0 3 10
IEL
LPL
days p.i.

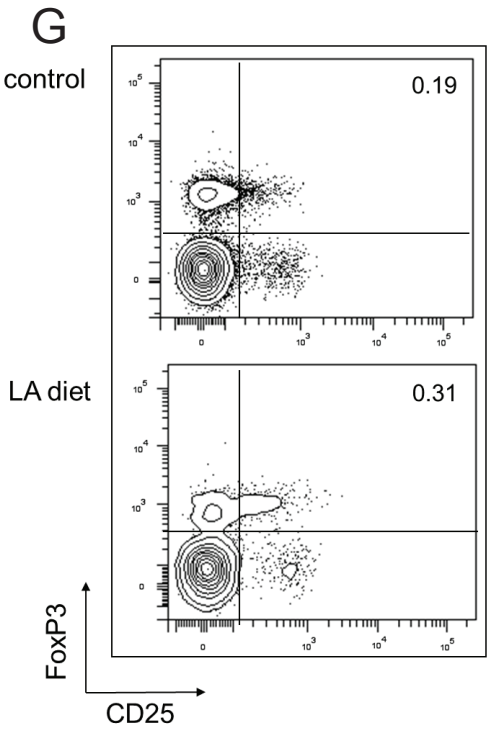
G
control
0.19
LA diet
0.31
FoxP3
CD25

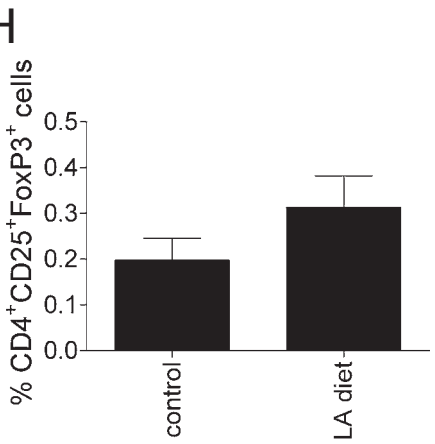
H
% CD4+CD25+FoxP3+ cells
0.5
0.4
0.3
0.2
0.1
0.0
control
LA diet

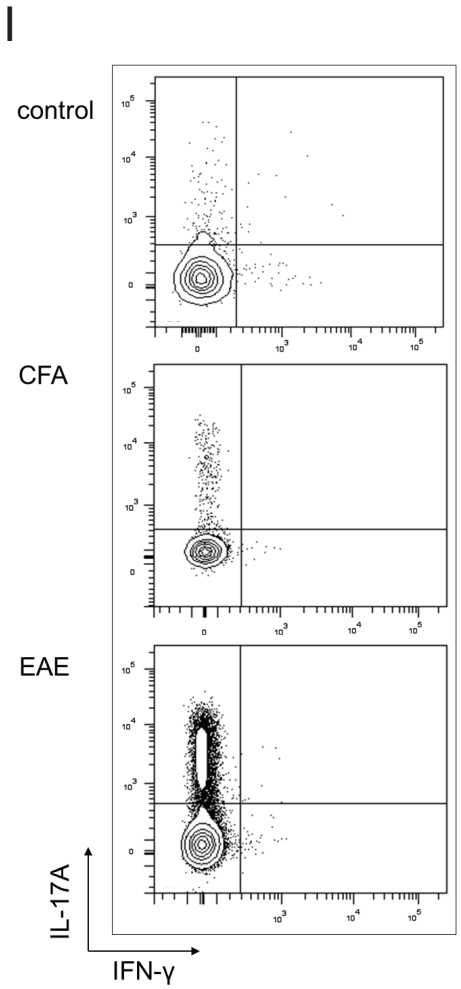
I
control
CFA
EAE
IL-17A
IFN-γ

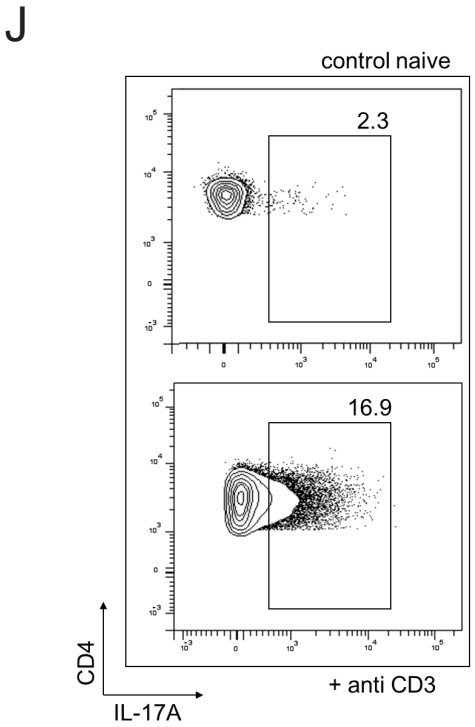
J
control naive
2.3
16.9
CD4
IL-17A
+ anti CD3

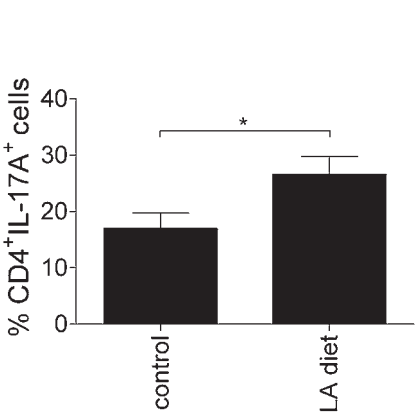
K
% CD4+IL-17A+ cells
40
30
20
10
0
*
control
LA diet

Supplemental Figures Legends

Supplemental figure S1, Related to Figure 1; LCFAs promote polarization of naïve T cells towards Th1 and Th17 cells. Consequences of LA on Th17 (A-D), Th1 (E-H) and Treg (1I-L) development in murine T cells. Naïve murine CD4+ T cells were cultured in normal medium or medium containing additional 250 μM LA and stimulated for 96h with anti-CD3, anti-CD28 and polarizing cytokines. Cell divisions, as determined by dye-dilution and intracellular production of cytokines, were analyzed simultaneously by Flow cytometry. Cell growth , cell death , apoptosis and frequencies of T cells were analyzed from parental (P) generation to the filial generations F1-F4, n=3 per group, data are presented as mean ± SEM, **p<0.01; ***p<0.001.

Supplemental figure S2A-C, Related to Figure 1; LCFAs promote polarization of naïve T cells towards Th1 and Th17 cells. (A-B) Microarray analysis of Th1 (n=4) and Th17 (n=5) differentiated CD4+ T cells following addition of LA versus control (triplicates, data pooled from two preparations, **p<0.01; ***p<0.001, unpaired t-test). (2C) Gene expression analysis of *Foxp3* expression of Treg-differentiated CD4+ T cells following addition of LA versus control (triplicates, data pooled from two preparations, *p<0.05, unpaired t-test).

Supplemental figure S2D, Related to Figure 2; MAPK pathways are modulators of LA cellular mechanism. mRNA expression analysis of LXRa, GPR40, 41, 43, 84, 119 and 120 via PCR in naïve T cells, Th0 cells, Th1 cells, Th17 cells, and Treg. H_2O denotes water control, M denotes fragment length marker. β-actin was used as a loading control.

Supplemental figure S3, Related to Figure 3; SCFAs promote polarization of naïve T cells towards Treg cells and suppresses the JNK1 and p38 pathway. qRT-PCR analysis of *lpin2, mapk8* and *mapk8ip2* expression in Th1 cells (A), Th17 cells (B), and Treg (C) after addition of 250 μM LA to differentiation culture versus controls (3 replicates, mean ± SEM, *p<0.05).

Supplemental figure S4, Related to Figure 4; LA exacerbates CNS autoimmunity and increases Th1 and Th17 cells *in vivo.* EAE in mice under a palmitate (C16:0)-rich diet. All data are presented as mean ± SEM, * $p<0.05$, Mann-Whitney U test. (A) Clinical course of MOG_{35-55} EAE, n=13 versus 15 mice. (B) Blinded quantification of Mac-3^+ macrophages/microglia in the spinal cord on day 20 p.i. (n=3 versus 5 mice). (C) Blinded quantification of $CD3^+$ T cells in the spinal cord on day 20 p.i. (n=3 versus 5 mice). (D) Analysis of IFNγ (A) and IL-17A (E) secretion in supernatants of splenocyte recall assays from EAE mice under LA or control diet by ELISA (day 10 p.i., n=5 per group,
one out of two experiments is shown, data are given as mean ± SEM, *$p<0.05$).

Supplemental figure S5, Related to Figure 5; LA exerts effect on Th17 cells via the small intestine. Quantification of MC-/LCFAs in the whole SI (A), duodenal mucosa (B), plasma (C), and blood cells (D) of mice on a control or LA-diet on day 10 post EAE induction (n=4 per group; mean ± SEM, *$p<0.05$, **$p<0.01$). Analysis of IL-17A (E) and IFNγ (F) production in anti-CD3- and anti-CD28-stimulated cultured intraepithelial lymphocytes (IEL) and lamina propria lymphocytes (LPL) from the colon on day 0, 3 and 10 of MOG_{35-55} EAE by ELISA (n=6 per group for day 0 and n = 4 per group for day 3 and 10 p.i., data are pooled from 2 different experiments. Data are shown as mean ± SEM, unpaired t-test). (G,H) *Ex vivo* flow cytometry analysis of small intestine LPL $CD4^+CD25^+$ $Foxp3^+$ Treg on day 10 of EAE after feeding a LA-rich versus control diet. (G) Representative contour plot from a mouse under LA-rich versus control diet depicting intracellular staining for Foxp3 versus CD25 after gating for $CD4^+$ T cells. (H) Quantification of $CD4^+CD25^+$ $Foxp3^+$ Treg. Data are shown as mean ± SEM. (I) *Ex vivo* flow cytometry analysis of small intestine LPL Th17 cells on day 10 of EAE versus naïve mice and CFA injection as controls. Representative contour plots are shown depicting intracellular staining for IFNγ versus IL-17A after gating for $CD4^+$ cells. (J). *Ex vivo* flow cytometry analysis of small intestine IEL Th17 cells on day 3 after injection of anti-CD3 antibody versus naïve mice as controls. Representative contour plots are shown depicting intracellular staining for IL-17A versus CD4. (K) *Ex vivo* flow cytometry analysis analysis of

Th17 cell frequencies in small intestine IEL after anti-CD3 antibody mediated injection. Data are pooled from two experiments, n=8 per group, unpaired t-test.

Supplemental Tab. 1; Related to Figure 5; LA exerts effect on Th17 cells via the small intestine.

Annoations of the operational taxonomic units which were most drastically down-regulated under LA diet.

Supplemental Table 1.

taxa id	phylum	class	order	family	genus	species
3	Bacteroidetes	Bacteroidia	Bacteroidales	Prevotellaceae	Prevotella	97otu31731
20	Bacteroidetes	Bacteroidia	Bacteroidales	S24-7	94otu13307	97otu14964
675	Nitrospirae	Nitrospira	Nitrospirales	Nitrospiraceae	94otu14268	97otu15924
35	Spirochaetes	Spirochaetes	Spirochaetales	Spirochaetaceae	Treponema	primitia
729	Euryarchaeota	unclassified	unclassified	unclassified	unclassified	unclassified
485	Planctomycetes	Planctomycetia	Pirellulales	Pirellulaceae	unclassified	unclassified
697	OD1	ABY1	85otu2364	unclassified	unclassified	unclassified
436	Bacteroidetes	Bacteroidia	Bacteroidales	S24-7	94otu3029	97otu19724
508	Proteobacteria	Alphaproteobacteria	unclassified	unclassified	unclassified	unclassified
175	Planctomycetes	Planctomycetia	Pirellulales	Pirellulaceae	94otu10318	unclassified
400	Acidobacteria	Acidobacteria	Acidobacteriales	Koribacteraceae	Candidatus Koribacter	unclassified
668	Firmicutes	Clostridia	Clostridiales	Lachnospiraceae	Coprococcus	unclassified

Supplemental Experimental Procedures

Mice, high-fat diet and EAE induction. Mice were initially purchased from Charles River (Sulzfeld, Germany), subsequently bred in-house, and then backcrossed on C57BL/6 background for at least 10 generations. All mice were housed at the in-house animal care facility of the University of Erlangen or at the Ruhr-University Bochum under a 12 hour day-night-cycle and standardized environment. For EAE, a power calculation was performed (G*Power Freeware, Version 3.1.5). To detect a one point difference on a 1-5 point scale with an alpha error probability of < 0.05 and a beta of > 0.95 and standard deviations representing up to 33% of the mean, the minimal number needed to analyze is n=8 per group resulting in an actual power of 0.951. For experiments under LA-rich diet conditions, mice received a chew containing 30.9 % crude fat (ssniff EF R/M E15116-34), while mice on a normal diet (control) were fed a chew with 4.2 % crude fat (ssniff EF R/M Control E15000-04). The high-fat chew is rich in the medium chain fatty acid C12:0 (lauric acid, 13.47 %) or, in other experiments, the long chain fatty acid C16:0 (palmitic acid). Mice were adapted to high-fat chew for 4 weeks before EAE induction and had ad libitum access to food and water throughout the adaption and observation period. For experiments under the SCFAs PA, either 200 µl PA (150 mM) or the solvent (water) were applied daily via oral gavage in addition to normal diet with 3.3 % crude fat (ssniff V1534-000). PA was either given at the day of immunization (DI) or at onset of disease (OD). For transfer experiments, mice received either 200 µL PA (150 mM) or the solvent (water) via oral gavage in addition to normal diet for seven days before gut Treg were isolated (Miltenyi Biotec, Bergisch Gladbach, Germany) and injected ($5*10^5$ $CD4^+$ $CD25^+$ $Foxp3^+$ cells, i.p.) into EAE at the day of immunization.

For induction of EAE, male and female mice 8-11 weeks of age were anaesthetized (ketamine/xylazine 80 mg per kg/8 mg per kg) and received a total of 200 µg MOG_{35-55} and 200 µg CFA, containing 4 mg/ml *M. tuberculosis* (H37RA) administered by two subcutaneous injections of 50 µl emulsion left and right to the tail base. Pertussis toxin (200 ng/mouse) was applied intraperitoneally on days 0 and 2 p.i. The clinical evaluation was performed on a daily bases by a 5-point scale ranging from 0, normal; 1, limp tail, impaired righting; 2, gait ataxia;

3, paraparesis of hind limbs; 4, tetraparesis; 5, death. Mice were sacrificed if reaching a disease score of 4. All experiments were in accordance with the German laws for animal protection and were approved by both the local ethic committees of the University of Erlangen (AZ 54-2532.1-56/12) and the Ruhr-University Bochum (AZ 84-02.04.2014.A104).

For genetic deletion of the p38 alpha subunit, p38alpha$^{fl/fl}$ mice (Engel et al., 2005) on a C57BL/6 background were crossbred with CD4-cre mice as described previously (Kleinewietfeld et al., 2013).

For inhibition of p38/MAPK enzyme *in vivo*, mice were maintained on a control or LA-rich diet and received either 1 mg /kg/ d SB202190 (TOCRIS) intraperitoneally or vehicle from day −3 p.i. CNS leukocytes were isolated by percoll gradient centrifugation on day 17 p.i, stimulated by PMA/ionomycin and analyzed by flow cytometry for IL-17A and CD4 expression.

Splenic murine T cell culture and murine T cell differentiation. Splenic T cells were isolated by magnetic activated cell sorting (MACS) using the “pan T cell isolation kit II” according to the manufacturer’s instructions (Miltenyi Biotech). Isolated T cells were collected and re-suspended in MACS buffer at 3x10^7 cells/ml. For APC free differentiations, cells were fluorescently stained for 30 min in an antibody cocktail containing αCD4-FITC (RM4-5, eBioscience), αCD44-PE (IM7, BioLegend), αCD62L-APC (MEL-14, eBioscience) and αCD25-PE-Cy5 (PC61.5, eBioscience) and were subsequently isolated by fluorescence activated cell sorting on MoFlo (Beckman-Coulter) in the FACS-core unit in Erlangen. For Th17 differentiation, sorted naïve T cells ($CD4^+CD62L^+CD44^{low}CD25^-$) were stimulated by plate-bound anti-CD3 (2 µg/ml, 145-2C11, BD Pharmingen) and anti-CD28 (2 µg/ml, 37.51, BD Pharmingen) in the presence of either IL-6 (40 ng/ml) and TGFβ1 (1ng/ml) or IL-6 (40 ng/ml) and IL-23 (10 ng/ml) and were cultured for 4 days. For Th1 differentiations, naïve $CD4^+$ T cells were cultured for 96 h in a CO_2 incubator (37°C, 5% CO_2) with anti-CD3, anti-CD28, IL-12 (20 ng/ml) and anti-IL-4 (10 mg/ml, 11B11, BioLegend). For Treg differentiations, anti-CD3, anti-CD28, and rhTGF-β1 (1 ng/ml) were added to culture media. Th0 cells were obtained by the addition of anti-IL-4 (10 µg/ml) and anti-IFNγ (10 µg/ml). To determine the influence of fatty acids on T cell differentiation and proliferation, cells were

cultured with and without 250 µM or 500 µM LA, 150 µM PA, or other fatty acid derivatives (C4:0, C6:0, C8:0, C10:0) at a concentration ranged from 1µM to 10mM in stepwise ten-fold manner for 4 days. To approximate the physiological trafficking of fatty acids *in vivo* and to overcome hydrophobicity, LA was coupled to BSA. In some experiments, the specific inhibitor SB202190 (Sigma Aldrich) at concentrations of 5 mM or 1mM, the synthetic triacylated lipopeptide PAM3CSK4 (Invitrogen) at a concentration of 10 ng/ml, or sterile fecal filtrate was added to the cultures. For the latter, 200mg feces were re-suspended in 1ml ReMed and centrifuged, then adding 50µL of sterile filtered supernatant to T cell differentiation assay.

The growth of naïve T cells under high-fat conditions compared to that under normal diet conditions was determined by a daily flow cytometry analysis. Therefore, naïve T cells were cultured with plate-bound αCD3 (2 µg/ml) and soluble αCD28 (2 µg/ml) under Th0, Th1, Th17, or Treg conditions (see above). 0 (directly after seeding), 24, 48, 72 and 96 h after the seeding of the cells, three single replicates were harvested for flow cytometric analyses. To monitor proliferation, cells were labelled with fixable proliferation dye (eBioscience) according to the manufacturer's protocol.

For intracellular flow cytometry, cells were stimulated for 4 h with ionomycin (1 µM) and PMA (50 ng/ml) in the presence of monensin (2 µM) and stained for CD4 (RM4-5, eBioscience), intracellular IL-17A (eBio17B7, eBioscience), and IFNγ (XMG1.2, eBioscience). A fixable viability dye eFluor®780 (0.2 µl/test) was used to exclude dead cells. Treg cells were stained by using the FoxP3$^+$ Treg staining kit following the manufacturers' protocol (mouse regulatory T cell staining kit #1, ebioscience, San Diego, USA).

Human T cell differentiation. Peripheral blood was obtained from healthy control volunteers in compliance with Institutional Review Board protocols. Peripheral blood mononuclear cells (PBMCs) were separated by Ficoll-Paque PLUS (GE Healthcare) gradient centrifugation. Total CD4$^+$ T cells were isolated from PBMCs by negative selection via the CD4$^+$ T cell isolation kit II (Miltenyi Biotec) and stained for CD45RA (HI100, eBioscience), CD45RO (UCHL1, eBioscience), CD25 (2A3, BD Pharmingen), and CD127 (hIL-7R-M21, BD

Pharmingen). Naïve ($CD45RA^-CD45RO^+CD25^-CD127^+$) $CD4^+$ T cells were subsequently isolated by fluorescence activated cell sorting on MoFlo (Beckman-Coulter) in the FACS-core unit Erlangen, Germany. Naïve T cells were cultured in 96-well round-bottom plates (Costar) with $5.3x10^4$ cells per well in serum-free X-VIVO15 medium (BioWhittaker) or serum free LGM 3 Medium (Lonza) for 5 to 7 days and stimulated with both plate-bound anti-CD3 (10 µg/ml, OKT3, eBioscience) and soluble anti-CD28 (1 µg/ml, CD28.2, eBioscience). For Th1 differentiation, naïve T cells were cultured with recombinant IL-12 (10 ng/ml) and anti-IL-4 (10 µg/ml, 8D4-8, BioLegend). For Th17 differentiation, naïve T cells were cultured with IL-1β (12.5 ng/ml), IL-6 (25 ng/ml), IL-21, IL-23 (25 ng/ml), and rh-TGFβ1 (10 ng/ml). For Treg differentiation, naïve T cells were cultured with recombinant human TGFβ (5ng/ml, R&D). For investigating influence of PA on Treg differentiation, PA was added in range from 1µM to 10mM in ten-fold manner. Additionally Treg cells were stained with CellTrace™ CFSE Proliferation Kit (Invitrogen) according to manufacturer protocol. Where indicated, 250 µM BSA-coupled LA was added to the cultures. Cell cultures were incubated at 37^oC in a humidified atmosphere with 5% CO_2, Treg for 5 days, other cultures for 7. All cells were analyzed via flow cytometry analysis.

Isolation of CNS infiltrating lymphocytes. Brain and spinal cord of mice on high-fat or control diets were removed on day 14 p.i. and separately disrupted with a 5 ml glass homogenizer. Both tissues were strained through a 100 µm cell-strainer and sedimented by centrifugation (500g, 10 min, 4°C). Each cell sediment was re-suspended in 6 ml 30% isotonic Percoll™ and transferred into a 15 ml tube for a three-step density gradient. CNS infiltrating lymphocytes were harvested from the interphases, washed with cold PBS, and re-suspended in Re-medium for intracellular cytokine staining and *ex vivo* flow cytometry analysis.

Isolation of splenic lymphocytes. Spleens of mice on a high-fat or control diets were removed on day 10 p.i. and disrupted with a 5 ml glass homogenizer. The tissue was then filtered through a 100 µm cell-strainer followed by an erythrocyte lysis. After washing with cold DPBS, cells were processed by intracellular cytokine staining and *ex vivo* flow cytometry analysis.

Immune cell analysis in the gut. At different time points of EAE, single cell suspensions from lamina propria lymphocytes (LPL) and intraepithelial lymphocytes (IEL) were obtained using the Lamina Propria Dissociation Kit (Miltenyi, Bergisch Gladbach, Germany). To obtain single cell suspensions of IEL, gut pieces were de-epithelialized in a pre-digestion solution containing EDTA and DTT. LPL were obtained by enzymatic and mechanic dissociation of the intestinal pieces. Working steps were done according to the manufacturer's protocol. All isolated cell suspensions were re-suspended in DPBS for cell counting with trypan blue exclusion. Cytokines were determined via intracellular cytokine staining and *ex vivo* flow cytometry analysis or by ELISA after culture at a density of 10^5 cells/well for 2 days with plate-bound αCD3 (2 µg/ml, 145-2C11, BD Pharmingen) and soluble αCD28 (2 µg/ml, 37.51, BD Pharmingen).

Quantification of short chain fatty acids in feces. Short chain fatty acids were analyzed as described by Furusawa et al. (Nature 2013) with modifications. Briefly 10 mg of fecal samples were homogenized using 2.8 mm Precellys ceramic beads (Bertin Technologies) with extraction solution containing 100 ml 100 mM crotonic acid (Sigma) as internal standard, 50 ml HCL (Sigma) and 200 ml ether (Sigma). Samples were homogenized 10 min at room temperature at 1500 rpm on a shaker (Eppendorf) and followed by 10 min of centrifugation at 1000g. From the ether upper phase 80 ml was transferred into new glass vials containing 16 ml N-tert-butyldimethylsilyl-N-methyltrifluoroacetamide (MTBSTFA, Sigma). Samples were incubated for 20 min at 80°C shaken at 500 rpm on a shaker (Eppendorf) and left afterwards at room temperature for 24 hours for derivatization.

Immunohistochemistry and tissue staining. EAE mice were perfused with 4% PFA (paraformaldehyde, Sigma), and the spinal cords and spleens were removed and embedded in paraffin before sectioning in 5 µm slices. Luxol Fast Blue staining was performed for evaluation of demyelination, Bielschowksy silver impregnation for axonal integrity/damage. Immunohistochemistry was performed on 5 µm thick paraffin sections (αCD3 1:200; Serotec; Wiesbaden, Germany). Quantification of axonal preservation, cellular infiltrate, and degree of demyelination were performed in a blinded fashion on nine independent spinal sections per mouse. Cellular infiltrate was quantified by overlaying a stereological grid onto sections per

mm^2 white matter, and demyelinated areas semi-automatically by CellD Software (Olympus, Hamburg, Germany). Nine visual fields of the cervical, thoracic and lumbar spinal cord were used for quantification of axonal preservation counted on a 100 mm diameter grid.

Flow cytometry. *Ex vivo*-obtained CNS leukocytes, splenic lymphocytes, and intestinal lymphocytes were analyzed by staining for extra- and intracellular markers. Dead cells were excluded by a fixable viability dye eFluor®780 (0.2 µl/test). Nonspecific Fc-mediated interactions were blocked by addition of 0.5 µl αCD16/32 (93, eBioscience) for 10 min. For surface staining, cells were stained with the respective fluorochrome conjugated antibodies for 30 min in PBS. For intracellular cytokine staining, cells were stimulated for 4 h with ionomycin (1 µM) and PMA (50 ng/ml) in the presence of monensin (2 µM) for murine cells or 750ng/ml ionomycin and 50ng/ml PMA for 5 hours for human cells. Cells were stained for surface marker and made permeable by saponin buffer or Fix/Perm (eBioscience) according to the manufacturer's protocol. Intracellular cytokines were stained with the respective fluorochrome conjugated antibodies for 30-45 min.

Cytokine detection. Cytokine concentrations in cell culture supernatants were analyzed by enzyme-linked immunosorbent assay (ELISA) for the secretion of IL-17A, IFNγ, and IL-10 (eBioscience) according to the manufacturer's instructions.

Real-time PCR. Gene expression was analyzed by real time PCR in cultured cells. Cells were lysed in RLT-buffer (RNeasy kit, QIAGEN), and total RNA was isolated using the RNeasy kit following the manufacturer's instructions (QIAGEN). RNA yield was quantified by absorbance measurements at 260 nm. 50-500 ng of total RNA were used per reaction to reversely transcribe RNA into cDNA, using QuantiTect® transcriptases according to the protocols (QIAGEN). PCR reactions were performed at a 5 µl scale on a qTower real time PCR System (Analytic Jena) in triplicates. Relative quantification was performed by the ΔΔCT method, normalizing target gene expression either on *Actb*/β-Actin or Rn18s as housekeeping gene.

Western blotting. Cultured T cells were harvested in 1xRipa lysis buffer [10xRipa: 150 mM NaCl, 38.5mM SDS, 50mM Tris, 134mM SDOX, 0.5 mM EDTA, 1% NP40, complete

protease inhibitor cocktail Complete Mini and phosphatase inhibitor cocktail PhosStop (Roche Diagnostic GmbH, Mannheim, Germany)] and centrifuged at 10,000 rpm for 10 min. Protein concentration was determined with BC Assay Protein Quantitation Kit (Interchim), and equal amounts of proteins were analyzed by Western blotting. P38 protein was detected by using rabbit anti-p38 (Cell Signaling Technology, 1:500). Phosphorylation of p38 protein was detected by using rabbit anti-phospho-p38 (Cell Signaling Technology, 1:500). Mouse anti-β-actin (1:1000) was obtained from Millipore (clone C4). As pp38 positive or negative control, C-6 glioma cells with or without anisomycin treatment were used (Cell Signaling Technology). Goat anti-mouse Alexa Fluor 488 conjugated and goat anti-rabbit Alexa Fluor 647 conjugated secondary antibodies (1:1000, Invitrogen) were used. Detection was performed with the Fusion Capt Advance FX7.